BASIC GEOMECHANICAL PROPERTIES OF THE DAWSON BAY FORMATION

By

DWAYNE WALTON KROLL

A Thesis

Presented to the University of Manitoba

in Partial Fulfillment of the

Requirements for the Degree of

Master of Science in Civil Engineering

Winnipeg, Manitoba

November, 1987

Permission has been granted to the National Library of Canada to microfilm this thesis and to lend or sell copies of the film.

The author (copyright owner) has reserved other publication rights, and neither the thesis nor extensive extracts from it may be printed or otherwise reproduced without his/her written permission.

L'autorisation a été accordée à la Bibliothèque nationale du Canada de microfilmer cette thèse et de prêter ou de vendre des exemplaires du film.

L'auteur (titulaire du droit d'auteur) se réserve les autres droits de publication; ni la thèse ni de longs extraits de celle-ci ne doivent être imprimés ou autrement reproduits sans son autorisation écrite.

ISBN 0-315-44144-5

BASIC GEOMECHANICAL PROPERTIES OF THE DAWSON BAY FORMATION

BY

DWAYNE WALTON KROLL

A thesis submitted to the Faculty of Graduate Studies of the University of Manitoba in partial fulfillment of the requirements of the degree of

MASTER OF SCIENCE

© 1988

Permission has been granted to the LIBRARY OF THE UNIVERSITY OF MANITOBA to lend or sell copies of this thesis, to the NATIONAL LIBRARY OF CANADA to microfilm this thesis and to lend or sell copies of the film, and UNIVERSITY MICROFILMS to publish an abstract of this thesis.

The author reserves other publication rights, and neither the thesis nor extensive extracts from it may be printed or otherwise reproduced without the author's written permission.

To my parents and brothers

For their support and understanding

Which enabled me to procure this degree

While retaining my family

ACKNOWLEDGEMENTS

I would like to take this opportunity to thank several people for their part in making this work possible, especially Dr. Emery Lajtai for providing me with the opportunity to work on this project. His direction, patience, and advice has been greatly appreciated.

I would also like to thank Mr. Wojciech Grajewski for teaching me the technical skills needed in the laboratory work. I would also like to express my thanks to all of my friends and colleagues in the geotechnical group for their support and assistance.

The funding for this research was jointly provided by the Potash Corporation of Saskatchewan (PCS) and the Natural Science and Engineering Research Council (NSERC) and was greatly appreciated.

Finally, I would like to thank my Father and Mother, and my brothers, for supporting me with the love and encouragement I needed to make it through all of my academic years.

ABSTRACT

The geomechanical properties of the limestone members of the Dawson Bay Formation have been studied to provide strength and deformational parameters for both physical and finite element models examining the causes of mining induced seismic occurrences above some potash mines in Saskatchewan. The properties of the limestone analyzed were: the point load strength, compressive strength, tensile strength, triaxial strength, frictional resistance, long term compressive strength and deformation moduli. A new experimental method was also developed to find the tensile deformation moduli by indirect means.

The results from these tests vary widely, but indicate that the Dawson Bay limestone is very strong with an average uniaxial compressive strength (σ_c) of 110 MPa, a tensile strength (σ_t) of 10 MPa, a friction angle = 33 degrees, a Young's modulus (E_c) and Poisson's ratio (ν_c) in compression of 34100 MPa and 0.25 respectively and triaxial strength parameters m = 25.96 and s = 1 for the grey limestone and strength parameters of m = 8.14 and s = 1 for the brown limestone. The elastic moduli in tension are different from the elastic moduli in compression. From the Brazilian tests, it was determined that the average Young's modulus in tension is about 37% lower than the average Young's modulus in compression. The Poisson's ratio in tension was about 120% higher than Poisson's ratio in compression (ν_c). It was also determined that the strength of saturated Dawson Bay limestone is time-dependent with the static fatigue limit being as low as 20 MPa.

From these test results and from structural and geological logging of Dawson Bay core, enough information exists to model the Dawson Bay Formation. The Dawson Bay limestone should be modeled as a thick elastic beam approximately 40 m thick. The bedding planes should not be considered as planes of weakness within the beam, but a vertical joint system should be included.

TABLE OF CONTENTS

	Page
ACKNOWLEDGEMENTS	i
ABSTRACT	ii
TABLE OF CONTENTS	iv
LIST OF FIGURES	vi
LIST OF TABLES	ix
CHAPTER 1 - INTRODUCTION	1
CHAPTER 2 - GEOLOGY OF THE DAWSON BAY FORMATION	3
2.1 SECOND RED BED MEMBER	4
2.2 THE BURR MEMBER	10
2.3 THE NEELY MEMBER	13
2.4 HUBBARD EVAPORITE MEMBER	13
CHAPTER 3 - EXPERIMENTAL PROGRAM	14
3.1 POINT LOAD TESTING	15
3.2 UNIAXIAL COMPRESSION TESTS	16
3.3 STRAIN GAUGED UNIAXIAL COMPRESSION TESTS	17
3.4 BRAZILIAN TESTING	18
3.5 TRIAXIAL TESTING	20
3.6 DIRECT SHEAR TEST	23
3.6.1 Rock Type and Sample Preparation	23
3.6.2 Testing Equipment	24
3.6.3 Calibration of Pressure and LVDT Transducers	25
3.6.4 Final Set Up	26
3.7 STATIC FATIGUE TESTING	27
3.7.1 Introduction	27
3.7.2 Sample Preparation	27
3.7.3 Uniaxial compressive strength tests	28
3.7.4 Time to failure tests	28
CHAPTER 4.0 - EXPERIMENTAL TEST RESULTS	30
4.1 POINT LOAD TEST RESULTS	30
4.2 COMPRESSIVE STRENGTH RESULTS	34
4.3 COMPRESSIVE ELASTIC MODULI RESULTS	37
4.4 BRAZILIAN TEST RESULTS	42
4.5 TRIAXIAL TEST RESULTS	43
4.6 SHEAR TEST RESULTS	49
4.7 STATIC FATIGUE TESTING	50
4.7.1 Theoretical aspects of static fatigue testing	50
4.7.2 Modelling of Static fatigue data	51
4.7.3 Static fatigue limit	58

Page

CHAPTER 5.0 - INDIRECT TENSILE MODULI EXPERIMENTATION 60

5.1 THEORY 60
5.2 COMPRESSIVE MODULI 62
5.3 INDIRECT TENSILE MODULI RESULTS 63
5.3.1 Indirect tensile moduli results - K200DB Series . . . 65
5.3.2 Indirect tensile moduli results - K300DB Series . . . 68
5.3.3 Comparison of results from the different size Brazilian samples 68
5.3.4 Determination of compressive deformation moduli by indirect means 69

CHAPTER 6 - DISCUSSION 75

6.1 TEST RESULTS FROM OTHER SOURCES 75
6.1.1 Results from Queen's University 75
6.1.2 Results from CANMET 77
6.1.3 Saskatchewan Energy and Mines 78
6.2 COMPARISON OF RESULTS 79
6.3 INDIRECT TENSILE TEST RESULTS 82
6.4 STATIC FATIGUE RESULTS 86
6.5 STRUCTURAL MODELLING OF THE DAWSON BAY FORMATION 87
6.6 RECOMMENDATIONS FOR FUTURE TESTING 87

CHAPTER 7 - CONCLUSIONS 88

REFERENCES 90

LIST OF FIGURES

Figure		Page
Fig. 2.1	Location, outcrop and subcrop map of the Dawson Bay Formation (Dunn, 1982)	5
Fig. 2.2	Stratigraphic sequence of the Dawson Bay Formation	7
Fig. 2.3	Abrupt contact between the Prairie Evaporite Formation and the Second Red Bed (Note the irregularity of the contact)	8
Fig. 2.4	Heavily fractured nature of the Second Red Bed Member (The pens are positioned at slickensides)	9
Fig. 2.5	Abrupt contact between Burr member and Second Red Bed member (Note the thin laminae of oil shale at the contact at the bottom of the photograph)	12
Fig. 2.6	Photograph showing period of non-deposition, or hardground	13
Fig. 3.1	Point load test setup	18
Fig. 3.2	Uniaxial compression test set up	20
Fig. 3.3	Brazilian tensile test set up	22
Fig. 3.4	Triaxial compression test set up with using the Hoek cell	23
Fig. 3.5	Direct shear test set up	26
Fig. 3.6	Static fatigue test set up	30
Fig. 4.1	Point strength index data sheet	32
Fig. 4.2	Point load strength test size correction chart (CANMET, 1977)	33
Fig. 4.3	Variability of point load equivalent compressive strength through the Lanigan pilot hole core	34
Fig. 4.4	Relative frequency histogram of uniaxial compression test results	37
Fig. 4.5	Stress/strain curves for uniaxial compression sample K001DUS	39
Fig. 4.6	Stress/strain curves for uniaxial compression sample K002KUS	39
Fig. 4.7	Stress/strain curves for uniaxial compression sample K003DUS	40
Fig. 4.8	Stress/strain curves for uniaxial compression sample K004DUS	40
Fig. 4.9	Stress/strain curves for uniaxial compression sample K005DUS	41

Fig. 4.10 Stress/strain curves for uniaxial compression sample K006DUS 41

Fig. 4.11 Relative frequency histogram of Brazilian strength tests 45

Fig. 4.12 Spalling failure on an 89 mm Brazilian specimen 46

Fig. 4.13 Scatterplot of Triaxial test results showing two general trends 48

Fig. 4.14 Linear regression line of strength of Dawson Bay Limestone 57

Fig. 4.15 Linear regression line of time to failure data for Dawson Bay Limestone (load = 60 MPa) 57

Fig. 4.16 Weibull distribution plotted with strength data for Dawson Bay Limestone (N=17) 58

Fig. 4.17 Weibull distribution plotted with the time to failure data for the Dawson Bay Limestone at a constant stress of 60 MPa 58

Fig. 4.18 Time to failure results showing curve becoming asymptotic at low stress level 60

Fig. 4.19 Static fatigue curve for Dawson Bay limestone showing limiting trend for lower stress level 60

Fig. 5.1 Stresses and strains acting on an element at the center of a theoretical Brazilian test specimen 62

Fig. 5.2 Theoretical stress distribution along the vertical and horizontal dismeters of a Brazilian test specimen (Hondros, 1959) 65

Fig. 5.3 Stress/strain curve for typical Brazilian test 67

Fig. 5.4: Standard strain gauge arrangement on Brazilian sample . . 71

Fig. 5.5 Strain rosette arrangement on Brazilian sample 71

Fig. 5.6 Both the standard strain gauge arrangement and strain rosette give the same values for axial or compressive strain . . . 72

Fig. 5.7 Both the standard strain gauge arrangement and the strain rosette give similar values for the lateral or tensile st 72

Fig. 6.1 Variation of Young's modulus of elasticity in tension with tensile stress 84

Fig. 6.2 Variation of Poisson's ratio in tension with tensile stress 85

Fig. 6.3 Variation of Poisson's ratio in tension with tensile stress (smaller scale) 86

LIST OF TABLES

TABLE		PAGE
Table 2.1	Rock Quality Designation and rock quality (Hoek and Brown, 1980)	9
Table 4.1:	Uniaxial compressive test results	35
Table 4.2:	Compressive deformation moduli results	41
Table 4.3 :	Brazilian tensile strength test data	43
Table 4.4:	Triaxial compressive strength test data	46
Table 4.5:	Direct shear test results	50
Table 4.6:	Dry compressive strength of Dawson Bay Limestone specimens used in the static fatigue study	53
Table 4.7:	Time to failure results for Dawson Bay Limestone at a static fatigue stress of 60 MPa	54
Table 5.1:	Compressive moduli perpendicular to the bedding plane of the Dawson Bay Limestone	64
Table 5.2:	K200DB test data at low stress level (10 MPa)	67
Table 5.3:	K200DB test data at high stress level (20 MPa)	68
Table 5.4:	Mean indirect tensile moduli for high and low stresses (200DB series)	68
Table 5.5:	K300DB test data at low stress level (10 MPa)	70
Table 5.6:	K300DB test data at high stress level (20 MPa)	70
Table 5.7:	Mean indirect tensile moduli for K300DB test series	70
Table 5.8:	Indirect compressive deformation moduli from the K200DB test series	74
Table 5.9:	Indirect compressive deformation moduli from the K300DB test series	75
Table 6.1:	Inclination of boreholes used as sample sources for Queen's test program	76
Table 6.2:	Summary of Queen's test results	77
Table 6.3:	Unit classification of 84-2 core by CANMET (Gorski, 1986)	78

TABLE PAGE

Table 6.4: Mine rock strength test results (Gorski, 1986) 79

Table 6.5: Summary of uniaxial and Brazilian test results by CANMET (Gorski, 1986) 79

Table 6.6: Comparison of test results from different researchers on the Dawson Bay limestone 80

CHAPTER 1

INTRODUCTION

Canada has both the world's richest known potash deposits and some of the world's largest underground potash mines in the province of Saskatchewan. Mines have also come into production in New Brunswick, and feasibility studies are currently underway for an underground operation near Russell, Manitoba. While the long term outlook for Canadian potash is believed to be positive, the potash industry is highly competitive; strict control of mining costs is therefore necessary if profitability and competitiveness are to continue. One major underlying component of productivity is strata control. Two important problems associated with strata control experienced by the Saskatchewan Potash industry are mining induced seismicity and water infiltration.

Six minor seismic events have occurred at the Cory mine West of Saskatoon, the largest registering 3.1 on the Richter scale (Horner, 1983). Investigations initiated by the Potash Corporation of Saskatchewan (PCS) Mining Ltd., utilizing staff and facilities from the University of Saskatchewan, have proved beyond reasonable doubt that the earth tremors are mining induced seismic events. Gendzwill (1983) has determined that all of the earth tremors at the Cory mine have occurred at a shallow depth in the order of a kilometre, slightly above the mining horizon, within the Dawson Bay Formation. The concern is that these earthquakes might trigger major collapses resulting in loss of production, damage of the shaft and of surficial buildings, and in the worst scenario, loss of life.

A few potash mines are experiencing small amounts of water inflow, mainly from formation fluid and brine pocket sources. Several mines are also experiencing quite large inflows of water in the order of thousands of litres per minute. It is believed that the Dawson Bay Formation is an aquifer (Dr. P. Mottahed, per. com. 1987) and also acts, in conjunction with the underlying salt beds, as a seal between the mining zone and an even larger supply of brine in the superincumbent strata. It is feared that if the formation was heavily fractured, uncontrollable flooding would occur and result in the loss of the mine. In fact, the Potash Corporation of America Mine just outside of Saskatoon shut down its operations in January 1987 because of its inability to control the water inflow.

In order to understand the failure mechanism within the Dawson Bay Formation, a research program has been developed by the Civil and Geological Engineering departments of the University of Manitoba in conjunction with the Earth Sciences Department of the Potash Corporation of Saskatchewan, within the framework of an NSERC CRD research agreement. The research interests fall into three interrelated divisions:

i) laboratory determination of the mechanical properties of the potash and Dawson Bay Formation
ii) insitu testing of potash and the Dawson Bay Formation
iii) finite element numerical modeling of the problem

The scope of this thesis is concerned with the determination of the mechanical properties of the Dawson Bay Limestone, including:

i) Uniaxial compressive strength
ii) Brazilian tensile strength
iii) Compressive and tensile deformation moduli
iv) Triaxial strength
v) Point load strength
vi) Direct shear friction angle
vii) Time dependent strength

CHAPTER 2

GEOLOGY OF THE DAWSON BAY FORMATION

The carbonates, evaporites and mudstones, of the Dawson Bay Formation overlie the potash bearing Prairie Evaporite salt beds, and their geology is very important in the development of a model to evaluate the stress distribution imposed on the geological environment by the mining process. In the subsurface, the Dawson Bay Formation extends from eastern Alberta, across southern Saskatchewan and outcrops along Lake Winnipegosis in Western Manitoba (Fig. 2.1). The Dawson Bay Formation ranges in thickness from 184 ft (56 m) in the east, to 102 ft (31 m) in the west, and lies at an average depth of 2950 ft (900 m) in the north to about 3300 ft (1000 m) in the south (Dunn, 1982). There tends to be very little change in the lateral continuity of the lithological composition and stratigraphic thickness of the carbonate members. The formation is composed of four members:

1. Second Red Bed Member
2. Burr Member
3. Neely Member
4. Hubbard Evaporite Member

The interest in the geology of the Dawson Bay Formation, in this research, is confined mainly to the fractures, beds of weakness and unconformities, which control its structural integrity.

2.1 SECOND RED BED MEMBER

The Second Red Bed Member is the lowest member in the Dawson Bay

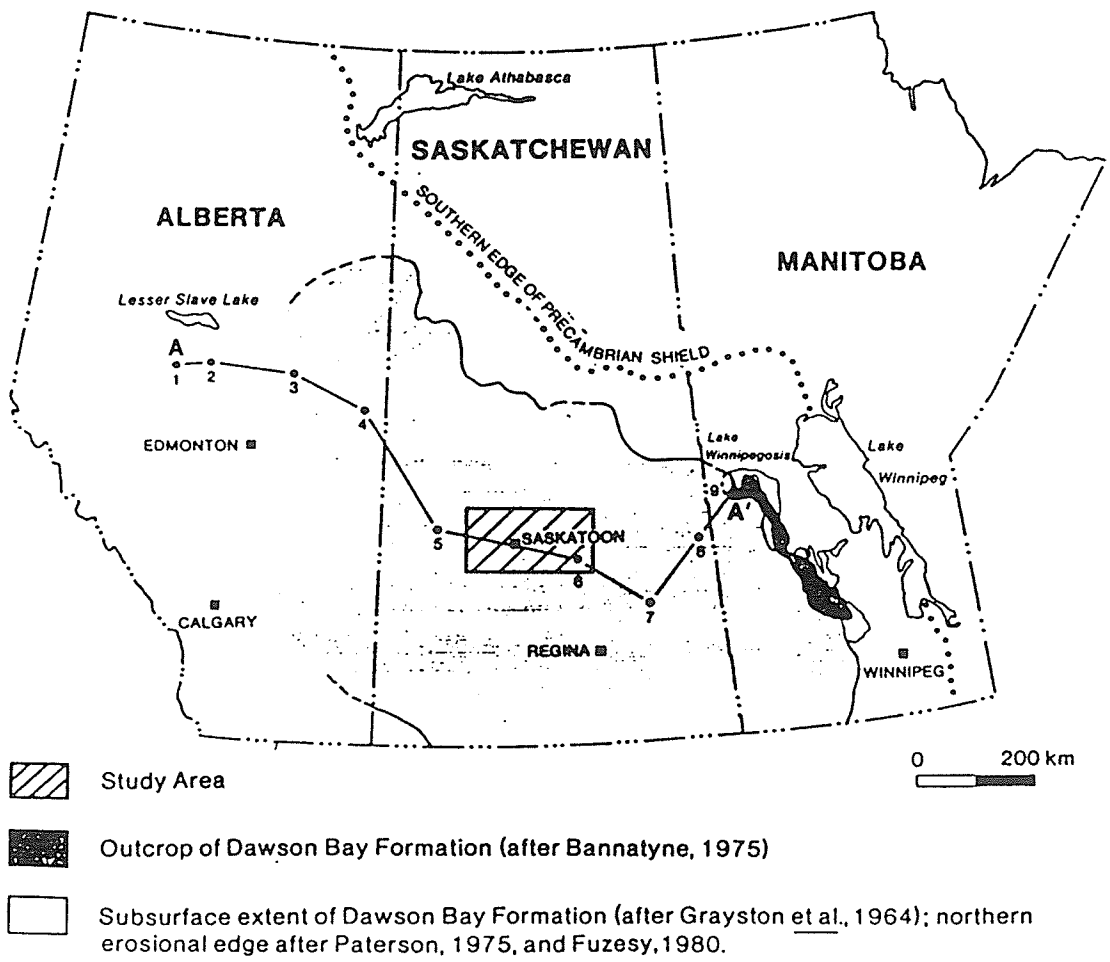

Fig. 2.1 Location, outcrop and subcrop map of the Dawson Bay Formation (Dunn, 1982)

Formation and in the Saskatoon area lies only 10m metres above the mining horizon (See Fig. 2.2). It is comprised of a non calcareous dolomitic mudstone resting with minor disconformity upon the salts of the Prairie Evaporite Formation. Dunn states that the contact is usually gradational in nature occurring over tens of centimetres. However, as shown in Figure 2.3, the contact in some areas is abrupt (Dunn, personal communication, 1985).

The thickness of the unit ranges between 10 ft (3 m) and 20 ft (6 m) but is usually about 14 ft (4.2 m). The dolomitic mudstone comprising the unit is red at the base, grading into brown , then grey at the top. Towards the top of the sequence, fractures are infilled with orange halite ranging in thickness from 2 mm to 30 mm. The heavily fractured poorly cohesive nature of the Second Red Bed Member makes it very weak and incompetent. The grey mudstone is commonly heavily fractured with slickensides yielding a Rock Quality Designation value for the member at less than 10% (Fig. 2.4). The Rock Quality Designation index (RQD), is a means of assigning a number to the quality of a rock mass based upon core recovery by diamond drilling. Proposed by Deere in 1964 (Hoek and Brown, 1980), the RQD is defined as the percentage of core recovered in intact pieces of 100 mm or more in length, as compared to the total length of the cored section examined. Hence:

$$\text{RQD (\%)} = 100 \times \frac{\text{length of core in pieces} > 100 \text{ mm}}{\text{length of cored section examined}}$$

The determination is simple, quick and inexpensive to implement if done in conjunction with normal geological logging. It offers an idea of the integrity of the rock mass as described in Table 2.1.

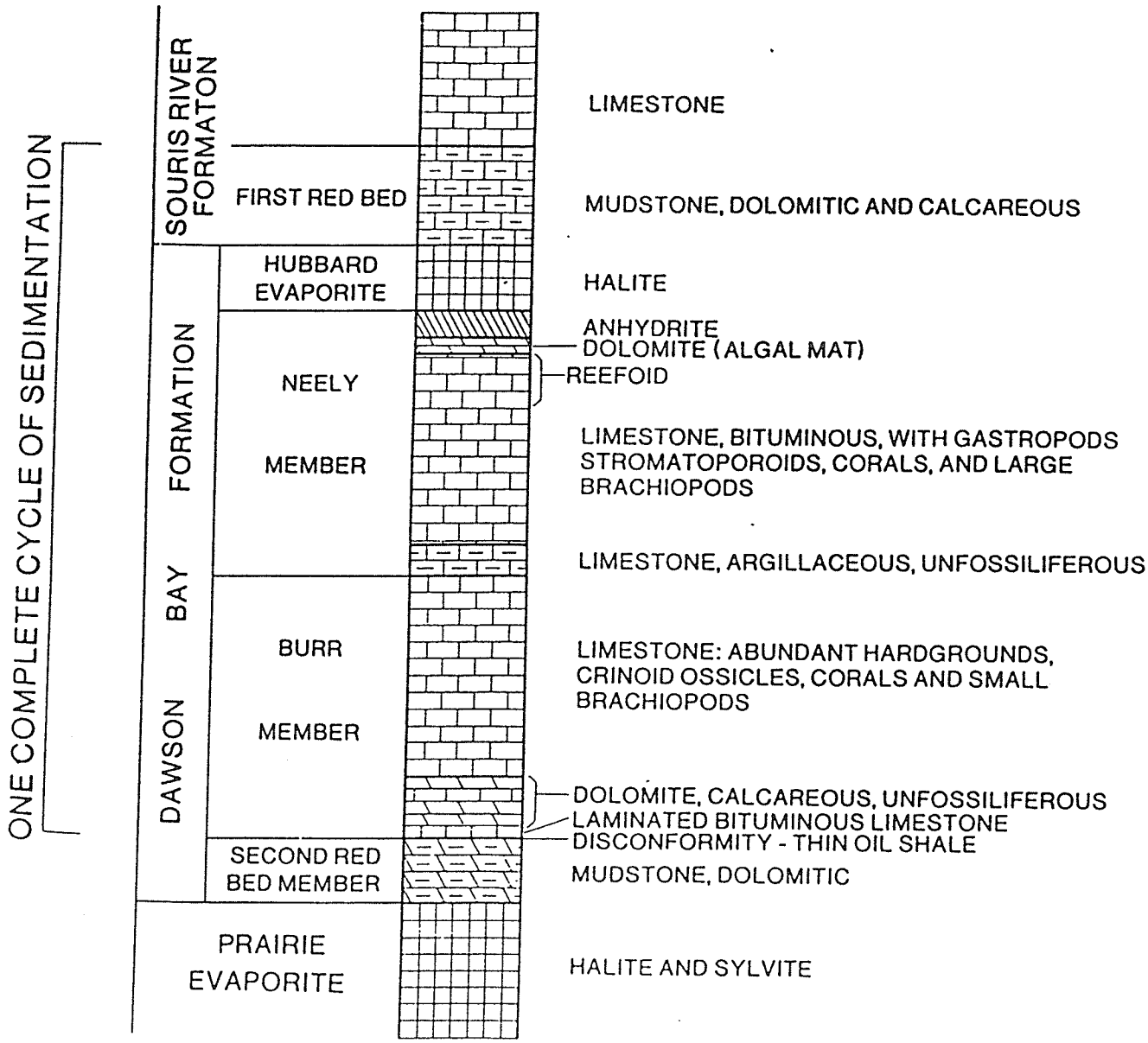

Fig. 2.2 Stratigraphic sequence of the Dawson Bay Formation (Dunn, 1982)

Fig. 2.3 Abrupt contact between the Prairie Evaporite Formation and the Second Red Bed (Note the irregularity of the contact)

Fig. 2.4 Heavily fractured nature of the Second Red Bed Member (The pens are positioned at slickensides)

Table 2.1 Rock Quality Designation and rock quality (Deere, 1964)

RQD	Rock Quality
<25%	very poor
25 - 50%	poor
50 - 75%	fair
75 - 90%	good
90 - 100%	very good

2.2 THE BURR MEMBER

The limits of the Burr Member are defined by the unconformity upon which it rests, separating it from the Second Red Bed member and the upper disconformity with the Neely member.

The member maintains a thickness of about 65 ft (20 m). The basal unconformity consists of 10 mm - 20 mm of oil shale followed by a distinct thin breccia (Fig. 2.5). The lower 10 ft (3 m) of this member is composed of a very fine grained dolomite with exfoliation of the core ,due to stress relief, noted in some of the cores. Five feet of dolomitic, microcrystalline bioturbated limestone lie directly on top of the dolomite. The upper part of the member is calcic limestone and is characterised by hardgrounds (Fig. 2.6). Hardgrounds are characterised by periods of non-deposition and burrowed erosional surfaces, but do not form planes of weakness. An argillaceous marker bed near the middle of the formation, which coincides approximately with the occurrence of the last of the hardgrounds, defines the boundary with the Neely member (Dunn, 1982). Core recovered from the Central Canada Potash mine near Saskatoon, shows fracturing within the last 18 ft (5 m) of the member. The joints are subvertical and most of them are infilled with white halite. Spacing between the joints varies between two and five feet (0.6 - 1.5 m). The Rock Quality Designation for this member is approximately 100%.

Fig. 2.5 Abrupt contact between Burr member and Second Red Bed member (Note the thin laminae of oil shale at the contact at the bottom of the photograph)

Fig. 2.6 Photograph showing period of non-deposition, or hardground

2.3 THE NEELY MEMBER

The Neely Member is also composed mainly of limestone and maintains a thickness between 50 and 60 ft (15 - 18 m). The bottom of the member is unfossiliferous and rests upon the last hardground of the Burr Member. Very fossiliferous layers of reefoid material are encountered moving upward, with intermittent wisps of bitumen. Thin bands of bitumen are located near the top. Four feet of anhydrite which caps the limestone signals the top of the Neely Member.

Although the thin laminae of bitumen and beds of fossils form or could cause relative planes of weakness, there is no indication of movement along them. In some cases, however, the core could be broken by hand at these planes of weakness. The Rock Quality Designation of the Neely Member is also approximately 100%.

2.4 HUBBARD EVAPORITE MEMBER

The top member of the Dawson Bay Formation is the Hubbard Evaporite Member. This translucent white and less commonly transparent bed is of variable thickness, up to 46 ft (14 m) (Dunn, 1982). In the core examined, however, this core was encountered for only a few feet.

CHAPTER 3

EXPERIMENTAL PROGRAM

Samples for testing purposes and geological core logging were obtained from three sources:

1. Central Canada Potash Mine
2. Subsurface Geological Laboratory in Regina
3. Lanigan Mine

The core samples varied in structure and composition along the length of all cores examined and it was impossible to get more than a few similar samples for any depth at any geographical location. This constraint arose from the tremendous expense of drilling to depths of one kilometre (the depth of the Dawson Bay Formation) and the reluctance of the mine operators to drill upward into the water bearing Dawson Bay Formation from the mining horizon. This apprehension stems from the fact that the Dawson Bay limestone is a barrier which separates the upper water bearing members from the Prairie Evaporite Formation and the mining zone. Any breach of this natural barrier could result in water inflow problems.

The samples obtained from the Central Canada mine site were taken from hole 84-2. A field trip was undertaken during the summer of 1985 to obtain the core, and at that time the author had the opportunity to tour the Central Canada Potash mine and visit their subsurface core shed where it was possible to log several other cores drilled into the Dawson Bay Formation from the mining level. The 42 mm borehole was drilled from the mining horizon, upward through the salt back, into the Dawson Bay Formation at an angle of 53 degrees from the horizontal. The total

length of the core was divided into three parts for testing by the Canada Centre for Mineral and Energy Technology (CANMET), Department of Geological Engineering University of Manitoba, and the Department of Mining Engineering Queen's University.

Samples obtained from the Subsurface Geological Laboratory were in the form of well core (89 mm diameter), from boreholes 13-25-32-24W Lanigan (PCS) and 5-10-23-32W Bredenbury (PCS). These and other cores were logged at the Subsurface Laboratory for their geological and structural properties.

Point load testing was performed and hand samples were obtained from the 66 mm pilot hole core at the Lanigan mine site.

The three different core sources enabled the author to test the Dawson Bay Formation over a large areal extent, making test results more relevant to the entire area covered by the Dawson Bay limestone as opposed to a localized area.

3.1 POINT LOAD TESTING

Axial point load tests were performed on core at the Lanigan mine site in order to evaluate the homogeneity of the geomechanical properties of the Dawson Bay Formation and to develop a relationship between results obtained from point load testing and uniaxial compressive strength results. The point load test has been successfully used previously in designing scale models of mine strata by converting the index results to uniaxial compressive values (Brook 1977).

Specimens were prepared and tested according to the guidelines set forth by CANMET (1977). Samples were prepared by breaking the 66 mm

diameter core into roughly 66 mm lengths; lengths in the range of 1.0 D +/- 0.1D were desired. Samples were then placed in a ROCTEST point load testing machine (Fig. 3.1) and a load was applied until the sample broke. At least seven samples were tested at each interval.

3.2 UNIAXIAL COMPRESSION TESTS

Simple uniaxial compression tests were conducted on core from Lanigan, Bredenbury and Central Canada Potash. The core from Lanigan and Bredenbury was originally 89 mm in diameter, from which three 31 mm diameter samples were cored. The samples from the Central Canada Potash core were 42 mm in diameter. All samples were cut and ends ground parallel and smooth, so that the length to diameter ratio was 2:1. The samples were then confined between two end platens with spherical seatings and placed in a BALDWIN-TATE 30000 pound universal loading machine. The samples were then quickly loaded until they failed. Thirty-four uniaxial compression tests were conducted in total.

3.3 STRAIN GAUGED UNIAXIAL COMPRESSION TESTS

Samples used in these tests were from the Central Canada Potash mine, borehole 84-2. The 42 mm diameter samples were cut using a commercial diamond saw. The ends were then ground parallel using a diamond wheel grinder so that the length of the sample was 84 mm. The surface of the sample was then sanded using a very fine grained sandpaper to remove dirt and dried drilling fluids, to ensure proper fixation of the strain gauges. Six 120 ohm, 5 mm long SHOWA steel strain gauges were attached to each sample using BEAN BR-610 ADHESIVE. Three gauges were

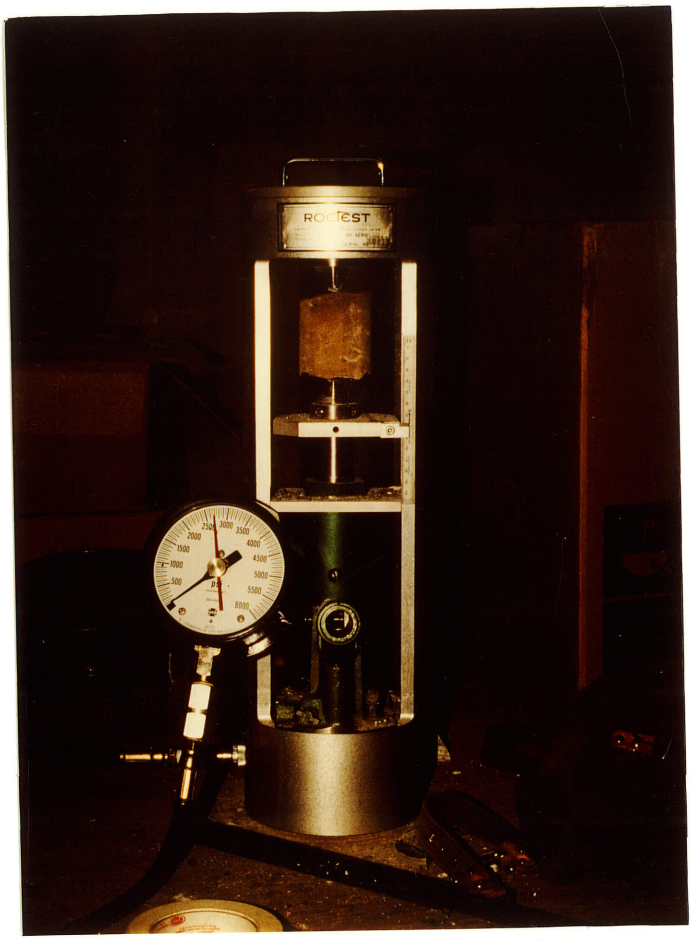

Fig. 3.1 Point load test setup

oriented parallel to the core axis to measure axial strain and three gauges were positioned perpendicular to the core axis to measure lateral strain. Both axial and lateral gauges were spaced at 120 degree intervals around the sample and within the middle third of the sample.

The samples were then allowed to cure in a laboratory oven at a temperature of 100 degrees Celsius for five hours. Wires were then soldered to the gauges, and the gauges protected by applying several coats of polyurethane. The wires were then connected to a VISHAY/ELLIS data acquisition system and the sample was set up in a BALDWIN-TATE-EMERY 30,000 pound universal loading machine (Fig. 3.2). The sample was loaded at a rate of approximately 500 pounds per minute with readings recorded on paper every 30 s. Six strain gauged samples were tested in total.

3.4 BRAZILIAN TESTING

As an alternative to the uniaxial tensile test, which is difficult to perform to acceptable standards for brittle materials (Mellor and Hawkes, 1971), diametral compression (Brazilian testing) of disks has strong appeal. The Brazilian test made on solid discs is appealing also for its simplicity in specimen preparation as compared to the expensive direct tensile test. In the experimental program, Brazilian disks were cut from two different core sizes; 42 mm diameter core and 89 mm diameter core. The diameter to thickness ratio of the 42 mm disks was approximately 1.7:1, while the ratio for the 89 mm disks was about 9:1. The 42 mm diameter samples were taken from the CCP 84-2 core, and the 89 mm samples were taken from borehole 13-25-32-24-W3 Lanigan and 5-10-23-32-W3 Bredenbury. Sample selection using the 42 mm core included

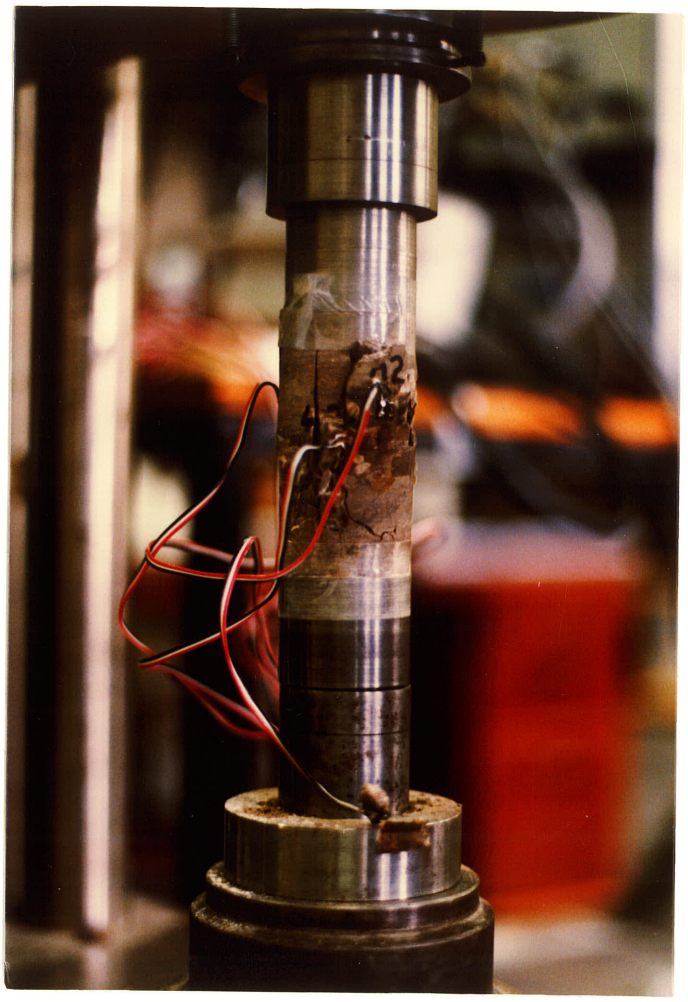

Fig. 3.2 Uniaxial compression test set up

specimens representative of both Dawson Bay limestone members. Sample ends were ground flat using a diamond grinder. The 42 mm samples were loaded in a set of curved steel platens to ensure that the intense stress concentration from point contact did not decrease the tensile strength of the sample (Mellor and Hawkes, 1971). The 89 mm diameter samples were taped with two layers of two sided tape at the platen - sample contact points to decrease point stress concentrations and were loaded in between two flat loading platens.

The 42 mm samples were strain gauged with four SHOWA 120 ohm steel strain gauges, 2 on each face; one oriented parallel to the axial stress, and one transverse to it (Fig. 3.3). The 89 mm diameter samples were fixed with both standard and strain rosettes. Wires were soldered to the gauges and connected to a VISHAY/ELLIS data acquisition system. Loading was applied at a rate of approximately 200 pounds per minute with the load and strain measurements recorded on paper tape. The sample diameter, thickness, footage and failure load were recorded.

3.5 TRIAXIAL TESTING

Triaxial testing was undertaken on the 42 mm diameter samples from the Central Canada potash core. Specimens were prepared as previously described with a length to diameter ratio of 2.0. Samples were lubricated using silicon oil then placed in a lubricated Hoek's cell. The sample was then set up in a 600,000 pound BALDWIN universal loading machine (Fig. 3.4). The confining stress was supplied by an air over oil system.

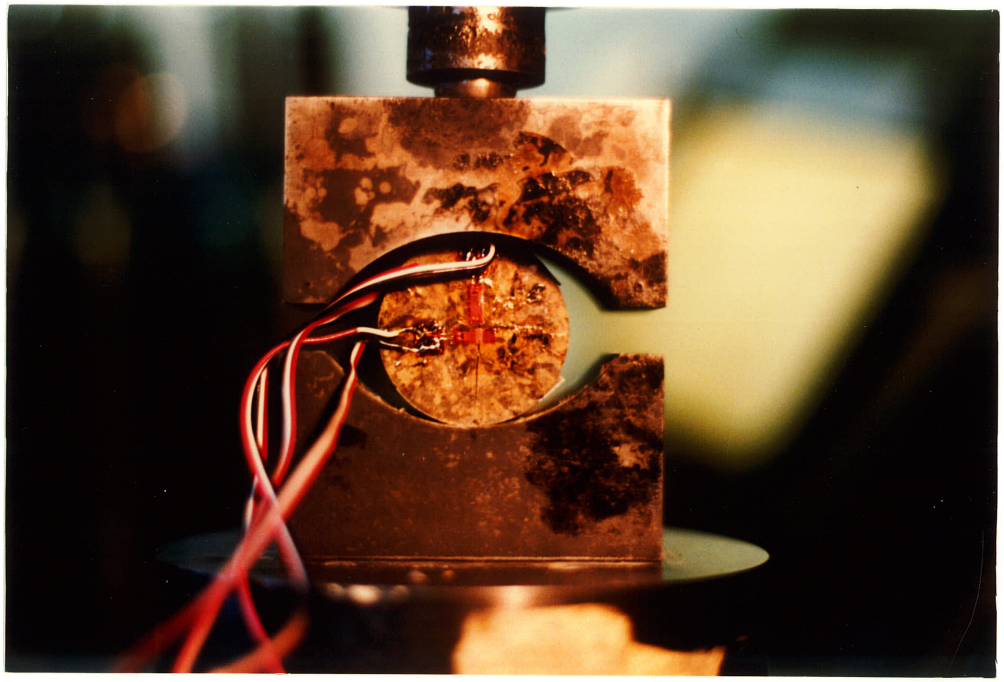

Fig. 3.3 Brazilian tensile test set up

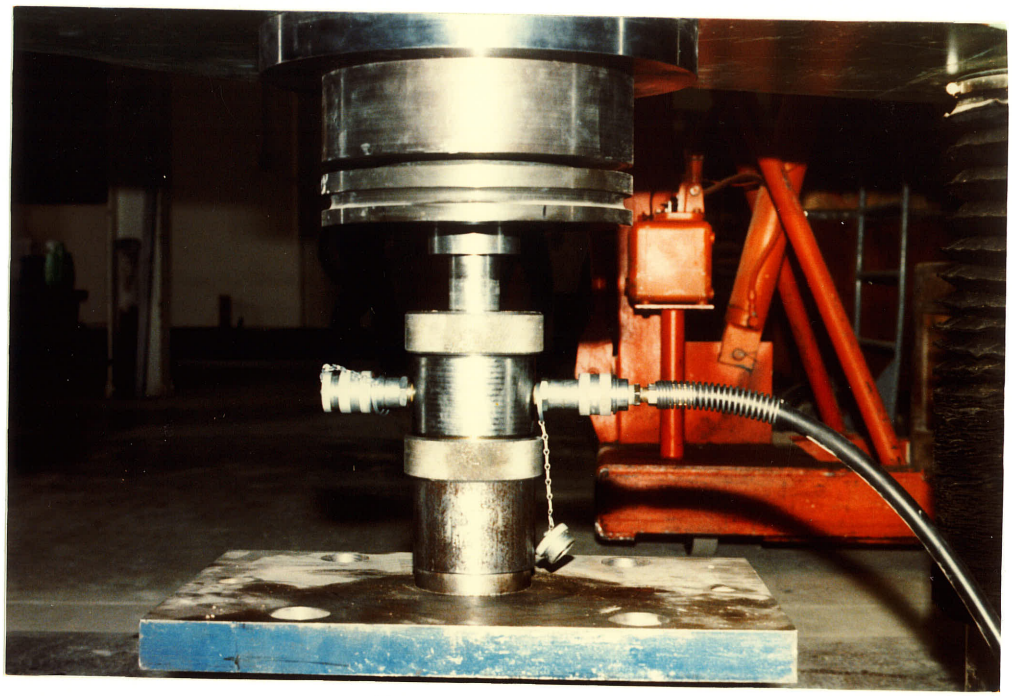

Fig. 3.4 Triaxial compression test set up using the Hoek cell

The lateral stress and the vertical stress due to loading were increased simultaneously to simulate hydrostatic conditions until the desired confining stress was reached. Six different confining pressures were used: 0, 10, 15, 20, 30, 40 MPa. After the desired confining pressure was reached, the axial load was increased at a rate of 250 pound per second (1.114 kN/s) until failure was reached. The sample diameter, confining stress, failure load, and angle of fracture were all recorded.

3.6 DIRECT SHEAR TEST

The strength of a rock mass will depend on the intact rock strength and frictional resistance along discontinuities. According to Barton (1971) it is first necessary to determine the basic friction angle in order to evaluate the frictional resistance of a discontinuity. This friction angle can be determined using the direct shear machine and a flat artificially prepared surface.

3.6.1 Rock Type and Sample Preparation

The sample used for the direct shear test was obtained from the Burr Member of the Dawson Bay Formation. It originated in the form of 89 mm core from the Bredenbury core. The microcrystalline limestone is light brownish grey in colour with crinoids, shells and other small fossils (to 2 cm).

The test specimens were cut with a diamond saw so that the face of the lower block of the specimen had the final dimension of 8.7 cm x 6.0 cm, while the face of the upper block had a dimension of 5.7 cm x 4.5 cm. The samples were cut and oriented so that the sliding surface modeled a

vertical joint occurrence, in situ. The two samples were then cemented into the upper and lower cylindrical boxes of the direct shear testing machine using a commercial grouting cement with a 3.5 : 1 cement to water ratio. The specimens were then ground flat using a commercial diamond wheeled grinder to ensure proper contact for the friction test. The sliding surface was not reground after any of the tests. Instead, a natural sliding surface evolved.

3.6.2 Testing Equipment

The RM 101 direct shear machine was used for this testing program. The machine was manufactured by the Structural Behaviour Engineering Laboratories Inc. (See Figure 3.5).

Two RAMs, RC-151 and RCH-121, manufactured by ENERPAC, were used for normal and shear loading respectively. The normal RAM has an effective area and maximum capability of 20.26^2 cm and 134 kN (15 tons), while the shear RAM has an area of 12.18^2 cm and a maximum capacity of 107 kN (12 tons). The normal RAM was connected to a pressure supply by means of a hydraulic hand pump. The loading supplied to the shear RAM was through an air hydraulic booster assembly.

Two pressure transducers were used to measure normal and shear loads. Displacement measurements were obtained by three HP7DCDT LVDTs (linear variable differential transducer): two read the vertical displacement and one the horizontal displacement.

3.6.3 Calibration of Pressure and LVDT Transducers

The pressure transducers in both the normal and shear loading

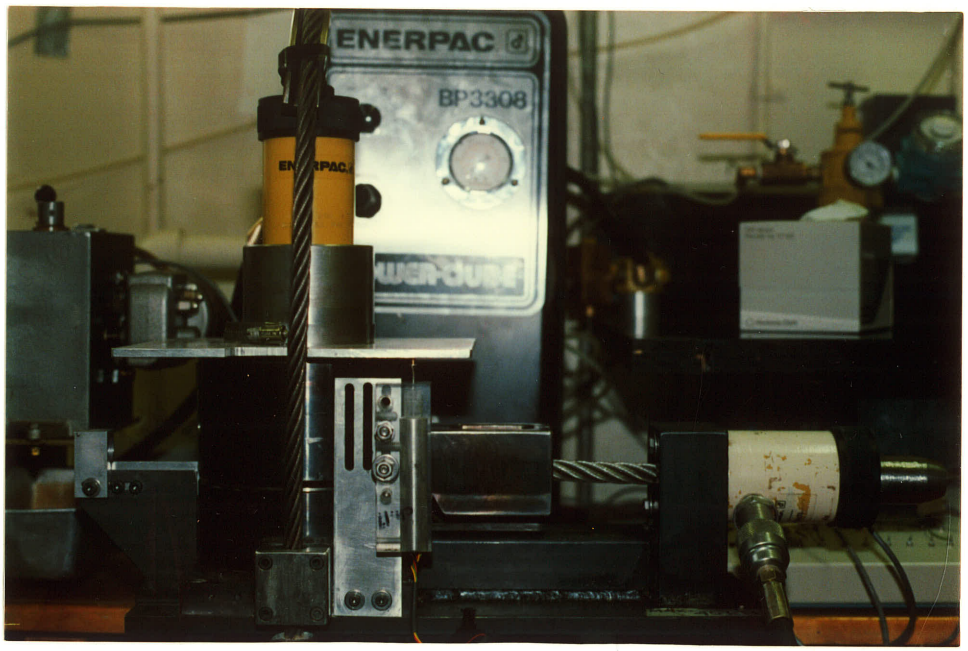

Fig. 3.5 Direct shear test set up

systems were calibrated using a universal testing machine. The calibration was done for a range of loads from 0 to 45 kN.

The horizontal and vertical displacements were measured by using LVDT transducers. These transducers were calibrated using a micrometer calibrator.

3.6.4 Final Set Up

After the calibration, the experimental set up was completed by connecting all LVDTs and pressure transducers to a Hewlett Packard (HP) Model 3421A data acquisition system, which transferred data to a HP75 micro computer. This computer was in turn interfaced with a HP9816 micro computer so that while the first one collected and stored the data, the second computer plotted the results on a monitor.

3.7 STATIC FATIGUE TESTING

3.7.1 Introduction

Static fatigue is defined as the delayed failure of a material under sustained loading. It has been recognized for some time as a problem involving underground excavations in rocks, but only recently it has been the object of experimental endeavour. This is mainly due to the interest in long term nuclear waste disposal studies (Schmidtke, 1986).

3.7.2 Sample Preparation

Two sample sources were used for the static fatigue testing program; borehole 13-25-32-14W Lanigan and 5-10-23-32W Bredenbury. The 89 mm diameter well cores were sawed into 90 mm lengths from which three

29 mm diameter samples were cored using a diamond drill bit and a slightly modified drill press. All samples were oriented parallel to the core axis. The drill was cooled and lubricated by a constant supply of water. The applied pressure, and consequently the speed on the bit, was controlled by the drill operator. Fifty-eight samples were cored in this fashion. All samples were numbered with ink, and their footage noted.

One edge of each sample was then ground flat using a grinder. Each specimen was then cut to a 60 mm length and ground flat to a length of 58 mm, giving a length to diameter ratio of 2:1.

3.7.3 Uniaxial compressive strength tests

The specimens were divided into two groups in a random manner. Compressive strength testing was performed on one set. The tests were carried out on a Baldwin hydraulically controlled testing machine with a capacity of 30,000 pounds. The specimens were loaded through hardened steel platens machined to a diameter of 29 mm. A spherical head was placed at one end to ensure even loading.

3.7.4 Time to failure tests

Static fatigue tests were carried out on the other set of specimens using a Structural Behaviour Engineering Laboratories CT-50 loading frame connected to an AP-1000 air on oil pump (See Figure 3.6). This equipment was able to supply a relatively constant uniaxial load to a specimen, +/- 5% (Schmitdke, 1986), until failure. Full load was transferred to the sample after a valve was opened for about two seconds.

The environmental conditions for the specimens in the static fatigue test were chosen to model those of the in-situ rock. Two plastic pails were filled with tap water and the specimens were immersed in them for a period of 24 hours. After that time it was decided that the samples should be placed in a brine solution which would resemble an environment more similar in chemical composition to the in-situ fluids. Pieces of potash were then pulverized and mixed with tap water to form a saturated brine solution. The samples were then transferred to the brine solution and remained there until the testing was completed. During testing, the samples were placed in a coated steel pot filled with water.

An important phenomenon noted during the testing of the limestone was that the samples seemed to "rot" when left to soak in the brine solution. In other words, the strength of the samples deteriorated to a level so that the second batch of test results could not be used in the analysis. Another important observation is that porosity played a key role in the time to failure tests. Test samples exhibiting very little porosity visually, yielded the longest time to failure.

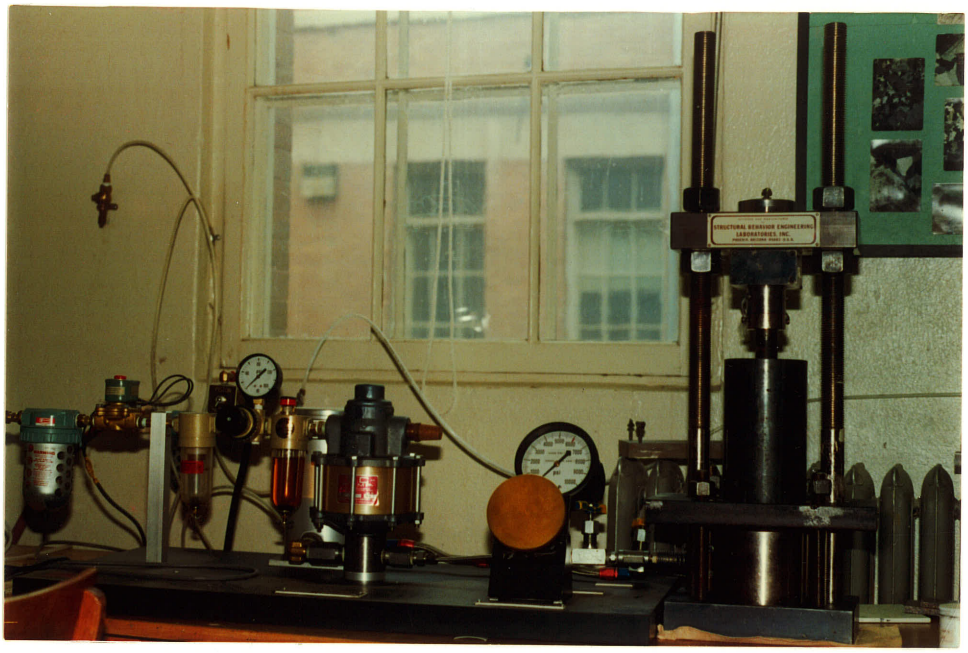

Fig. 3.6 Static fatigue test set up

CHAPTER 4.0

EXPERIMENTAL TEST RESULTS

4.1 POINT LOAD TEST RESULTS

The length of the specimen as well as the failure load were recorded and the point load strength index was calculated by dividing the effective load by the squared length of the sample (ROCTEST Manual, 1985) (See Fig. 4.1). The effective load is defined as the recorded pressure at failure multiplied by the effective area of the piston; which is 1.76 in^2 for the ROCTEST point load test machine. It has been noted by others (Broch & Franklin, 1972; Brook, 1977) that the point load index (Is) varies as a function of the diameter of the sample (D) in the diametral test, and as a function of the equivalent core diameter or length (De) in axial, block and irregular lump tests. A size correction must therefore be applied to obtain a unique point load strength index value for the rock that can be used for purposes of rock strength classification. The size corrected point load strength index Is is defined as the value of Is that would have been measured by a diametral test with D = 50 mm. The corrected Point Load Strength Index is calculated from the calculated strength index value using the conversion charts shown in Fig. 4.2. The median value (ROCTEST, 1985) of all the tests was then determined and multiplied by a factor of 24 (Brook, 1977) to obtain the equivalent compressive strength value.

Figure 4.3 shows the variation of the equivalent compressive strength (or point load strength), calculated from point load index testing, along the core. A minimum of seven point load tests were

POINT LOAD STRENGTH INDEX

Limestone, pale brown, halite inclusions,

Sample Some bituminous laminae. Date 85 07 08

Sample from about 12.5 ft above contact between Ist R.B. and Neely

Tested by D. Kroll

(Computed on: 85 07 16)

Location Alwinsal 3-28 (Lanigan)

Bore Hole Pilot Depth 3085

Average water content: - %

Sample No.

Average degree of saturation: - %

Test Type	Specimen No.	D (mm)	P (psi)	D^2 (in^2)	I_s	$I_s(50)$	Median Value	Notes
Axial	1	77	2550	9.19	488	575		Very hard to break
	2	74.5	2650	8.72	535	630		core for samples
	3	75	2575	8.72	520	620		to test, using
	4	63	2650	6.15	758	850		hammer & chisel.
	5	65	1900	6.55	511	580		
	6	69	2725	7.38	650	740	Is_{50}=	
	7	51	2400	4.03	1048	1050	620	
	8	58	1050	5.21	354	370		Don't forget to
	9	61	1300	5.77	397	420		reset gauge.

Median values of strength index, $I_s(50)$

Parallel to plane of weakness: _____ psi (_____ MPa)

Perpendicular to plane of weakness: 620 psi (4.25 MPa) σ_c=102 MPa

Anisotropy index, $I_a(50)$ = _____ = _____

Remarks: After finding all the $Is_{(50)}$'s, calculate the median and multiply this value by 24. The result will be your compressive strength σc.

4.25 x 24 = 102 MPa

Fig. 4.1 Point strength index data sheet

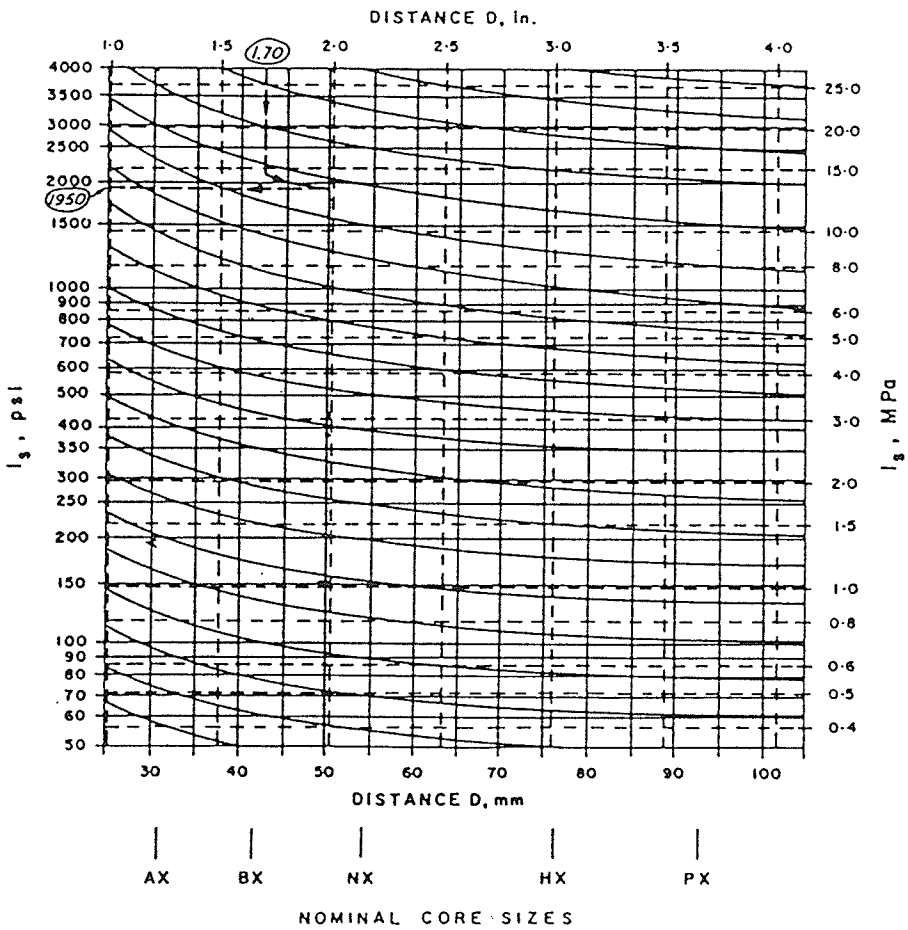

Fig. 4.2 Point load strength test size correction chart (CANMET, 1977)

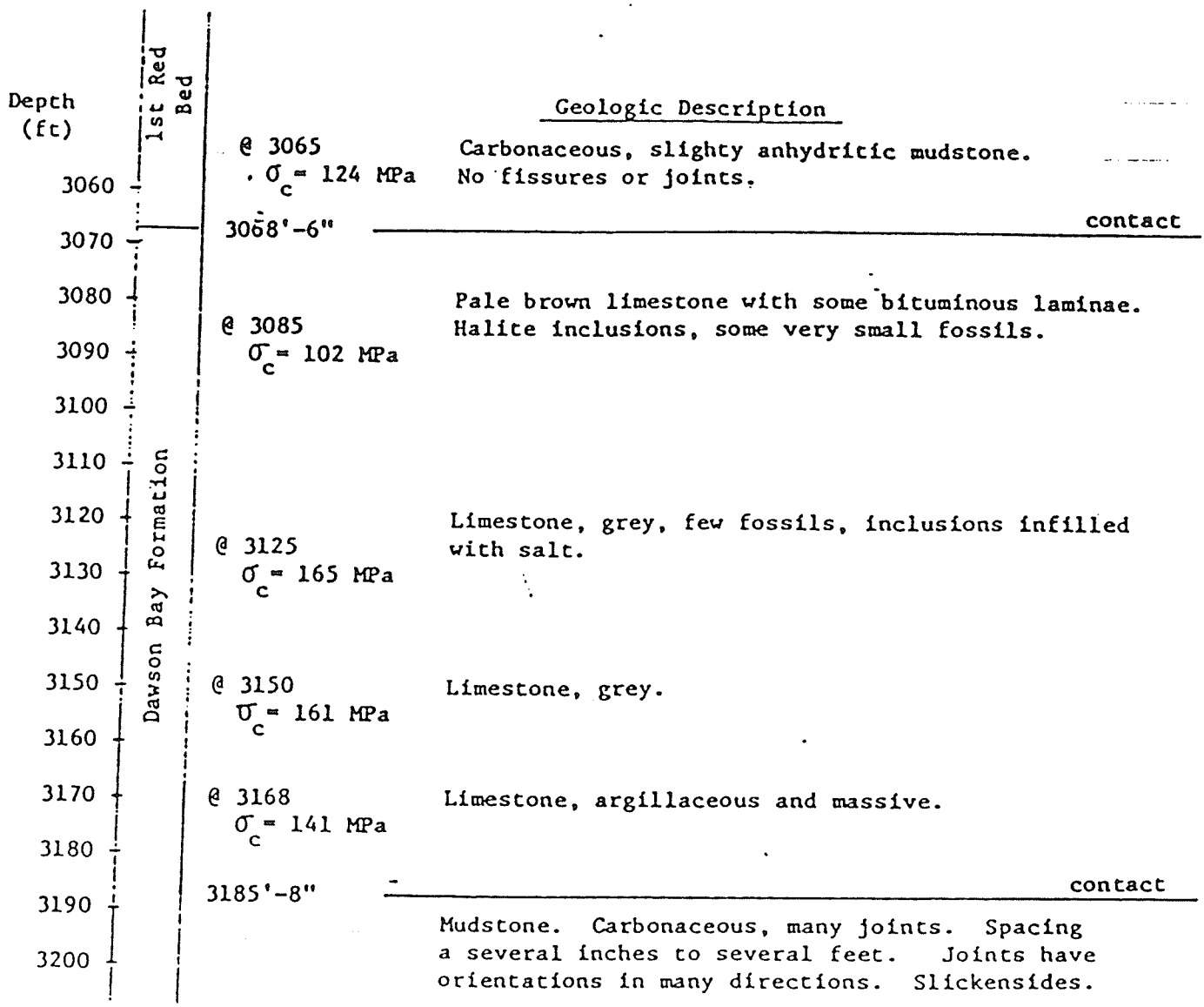

Fig. 4.3 Variability of point load equivalent compressive strength through the Lanigan pilot hole core

performed at each interval, with the amount of core in each interval being the limiting factor. The point load strength ranges from 102 - 165 MPa in the four sections tested, giving an average equivalent compressive strength (and standard deviation) for the Dawson Bay limestone of:

$$\sigma_c = 142 +/- 29 \text{ MPa}$$

4.2 COMPRESSIVE STRENGTH RESULTS

Table 4.1 shows the results of the uniaxial compressive testing. The results from the different diameter cores were converted to results that would theoretically be obtained from a 50 mm core by use of the empirical formula (Hoek and Brown, 1980) :

$$\sigma_{c50} = \sigma_u / (50 / D)^{.18} \qquad (4.1)$$

where: σ_{c50} = Compressive strength of a 50 mm diameter sample.
D = diameter of sample
σ_c = Compressive strength of a sample with diameter D.

The results are plotted in the form of a histogram in Figure 4.4. The mean compressive strength (σ_{c50}) for the tests is 97.84 MPa.

The results were then converted for a diameter to length ratio of 1:1 in order to compare with the results obtained by other workers using the formulae (DeSouza, 1986):

$$\sigma_c = \sigma_{c50} / (0.778 + 0.222(D / L)) \qquad (4.2)$$

where: σ_c = Uniaxial compressive strength of a sample with D/L = 1.0
D = Diameter of sample
L = Length of sample

The resulting mean compressive strength of the carbonate members of the Dawson Bay Formation is:

$$\sigma_c = 110.06 +/- 45 \text{ MPa}$$

Table 4.1: Uniaxial compressive test results

Sample	Core Source	Footage (feet)	Diameter (mm)	Load (kips)	σ_u (MPa)	Fracture Angle
K001DU	Lanigan	3246.4-3247.4	31	19.30	113.74	-
K002DU	"	"	"	13.20	77.79	-
K003DU	"	"	"	22.08	130.09	-
K004DU	"	"	"	21.50	126.71	-
K005DU	"	"	"	20.45	120.52	-
K006DU	"	"	"	20.50	120.81	-
K007DU	"	"	"	22.75	134.07	-
K008DU	"	"	"	21.35	125.82	78
K009DU	"	3264.4-3265.4	"	29.50	173.85	-
K010DU	"	"	"	29.50	173.85	-
K011DU	"	"	"	27.20	160.30	-
K012DU	"	"	"	27.20	164.72	-
K013DU	"	3271.0-3272.3	28	15.40	111.76	63
K014DU	"	3291.3-3292.3	"	14.60	105.97	-
K015DU	"	3300.5-3301.2	"	16.26	117.98	-
K016DU	"	3304.8-3305.8	"	23.61	171.36	-
K017DU	"	"	"	26.31	190.96	-
K018DU	BREDENBURY	2668.6-2669.6	"	10.54	76.50	66
K019DU	"	"	"	14.50	105.24	67
K020DU	"	2678.5-2679.5	"	8.16	59.19	-
K021DU	"	"	"	15.35	105.84	76
K022DU	"	"	"	9.15	66.41	67
K023DU	"	"	"	12.60	91.41	70
K024DU	"	2685.0-2686.0	"	9.25	67.14	-
K025DU	"	2708.0 2709.0	"	12.30	89.27	-
K026DU	"	"	"	10.89	78.93	-
K027DU	CCP. 84-2	112.8-114.0	42	25.31	81.20	-
K028DU	"	149.8-150.8	"	27.42	87.90	62
K029DU	"	157.8-158.8	"	12.48	40.00	63
K030DU	"	177.6-178.6	"	17.93	57.50	72
K002DU-S	"	63.0-64.5	"	27.78	38.53	-
K003DU-S	"	84.2-85.2	"	29.62	95.00	-
K004DU-S	"	103.0-104.0	"	19.36	62.10	-
K005DU-S	"	149.8-150.8	"	27.78	89.08	-

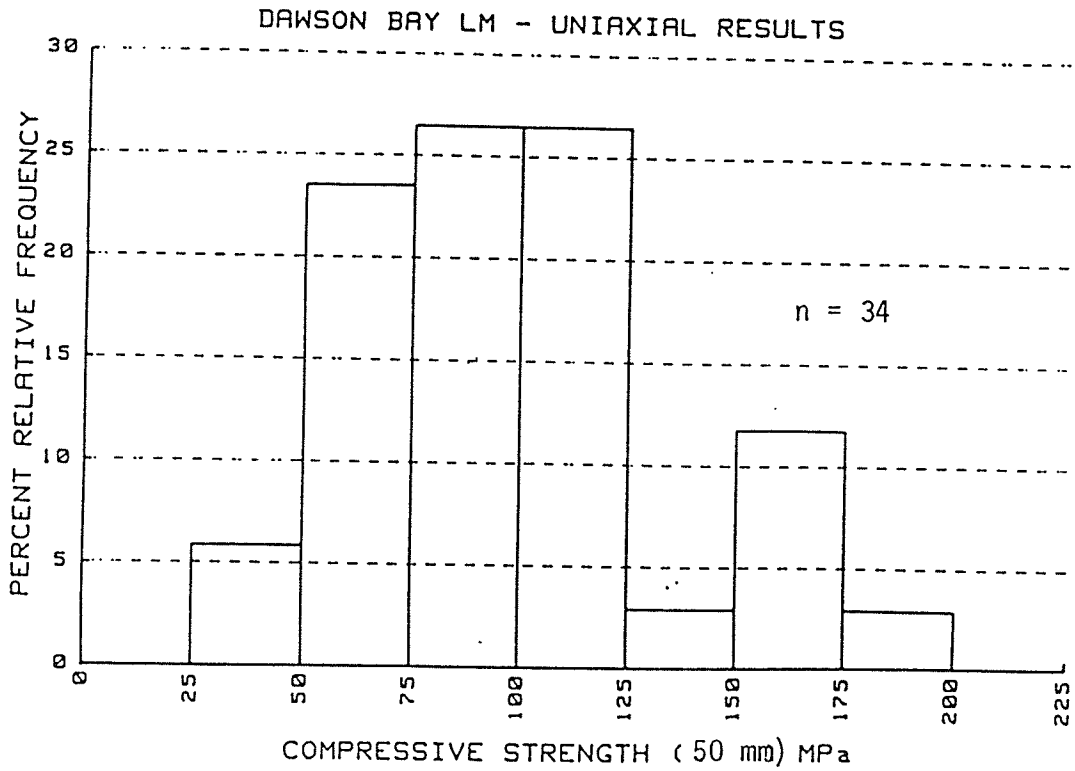

Fig. 4.4 Relative frequency histogram of uniaxial compression test results

4.3 COMPRESSIVE ELASTIC MODULI RESULTS

Results from the six strain gauged compressive tests are shown in Figures 4.5 - 4.10. The average values for both the axial and lateral strain gauges are presented, as well as the volumetric strain. The volumetric strain (Δ) in this case is defined as twice the absolute value of the lateral strain minus the axial strain, or:

$$\Delta = 2 * \varepsilon_1 - \varepsilon_a \tag{4.3}$$

The Young's Modulus of a sample is defined from Hoek's law as:

$$E = \frac{\text{Stress}}{\text{Axial Strain}} \tag{4.4}$$

Since strain is dimensionless, the modulus of elasticity (E) is expressed in the same units as stress. E was determined for each sample by taking the average slope, in the elastic portion, of each axial stress/strain curve (See Figures 4.5 and 4.6). As it can be seen, the stress/axial strain curve is rarely linear and therefore the quoted E is only a "best estimate".

In all materials, the compression produced by an axial force P in the direction of a force is accompanied by an extension in any transverse direction. This value is referred to as the lateral strain. When the conditions are elastic the absolute value of the lateral strain over the axial strain is called Poisson's ratio, after the French mathematician Simean Denis Poisson, 1781 - 1840 (Beer et al., 1981). The Poisson's ratio may be calculated by dividing the slope of the axial stress/axial strain curve by the slope of the axial stress/lateral strain curve. Table 4.2 gives the compressive deformation results for the strain gauged uniaxial compression tests. The average results for the compressive tests are:

$$E = 34100 +/- 10000 \text{ MPa}$$
$$\nu = 0.25 +/- 0.06$$

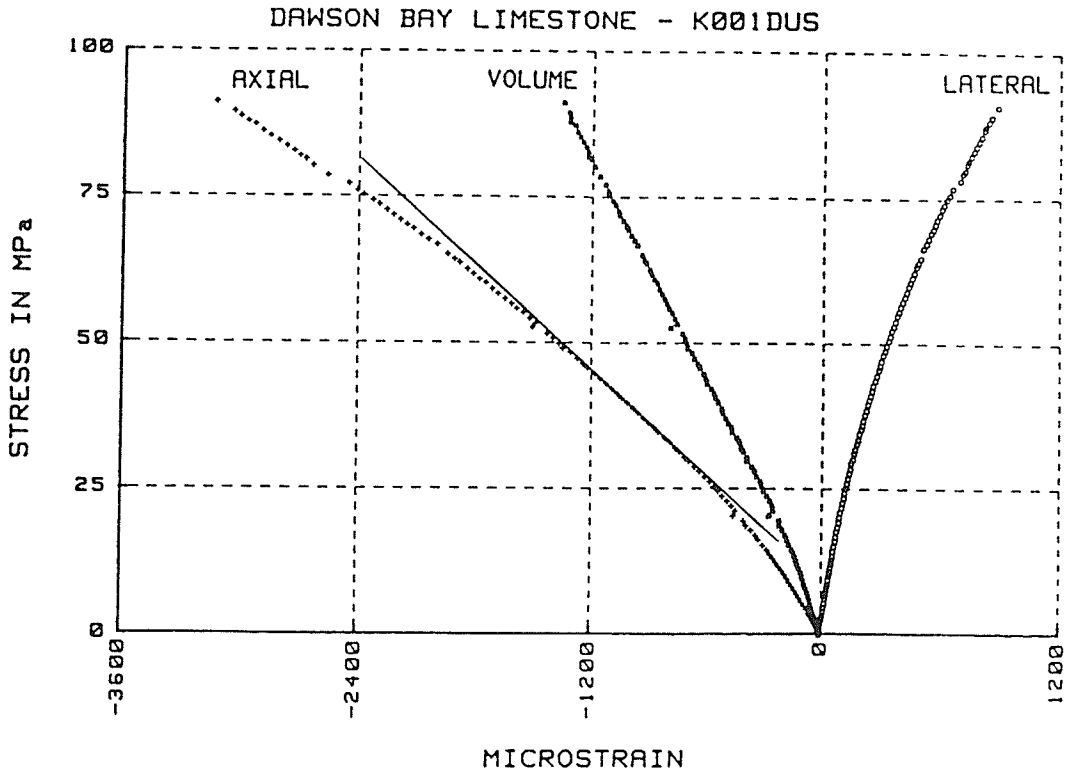

Fig. 4.5 Stress/strain curves for uniaxial compression sample K001DUS

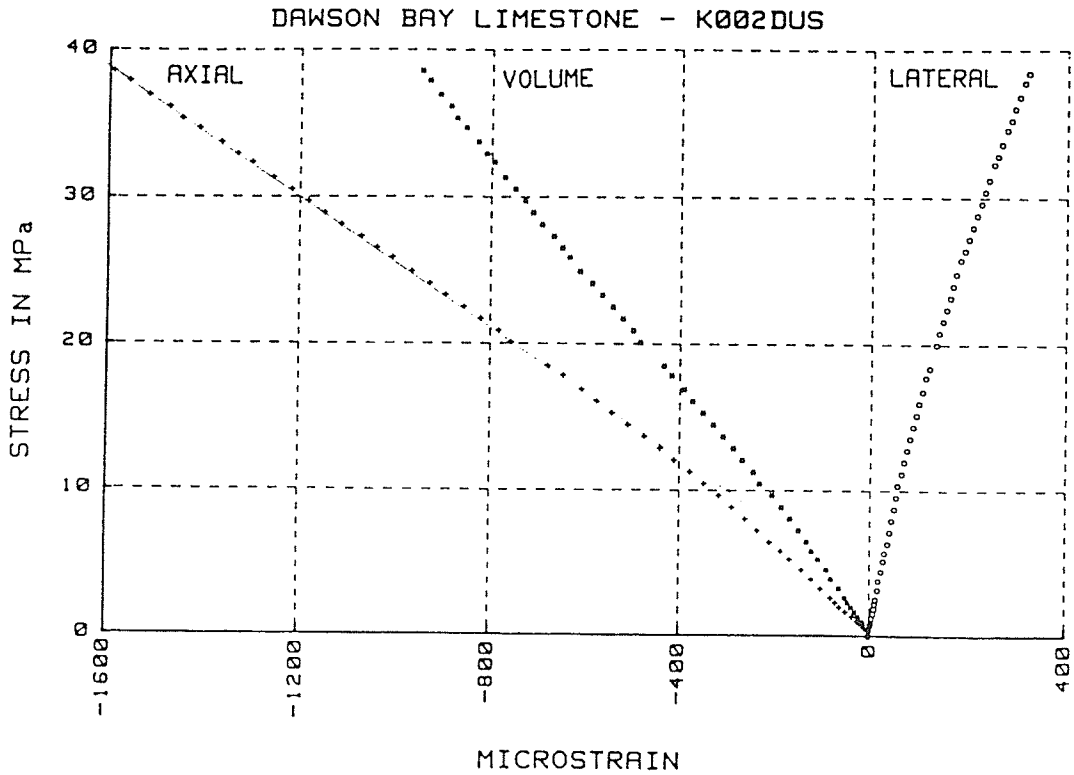

Fig. 4.6 Stress/strain curves for uniaxial compression sample K002KUS

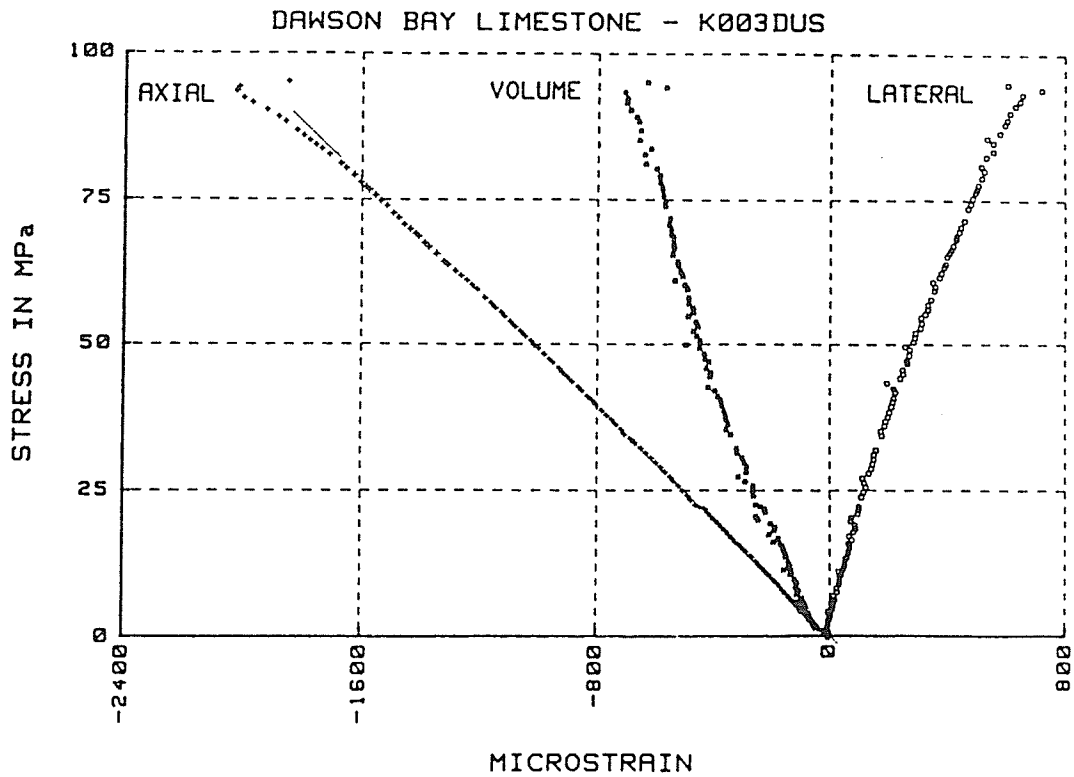

Fig. 4.7 Stress/strain curves for uniaxial compression sample K003DUS

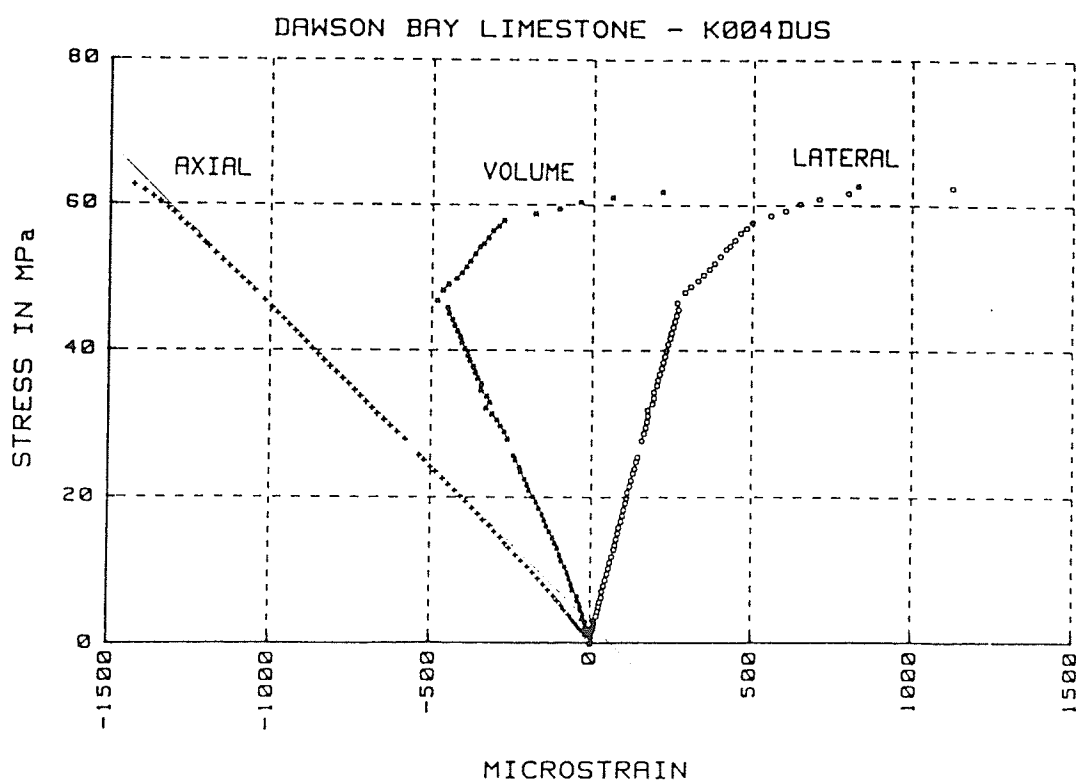

Fig. 4.8 Stress/strain curves for uniaxial compression sample K004DUS

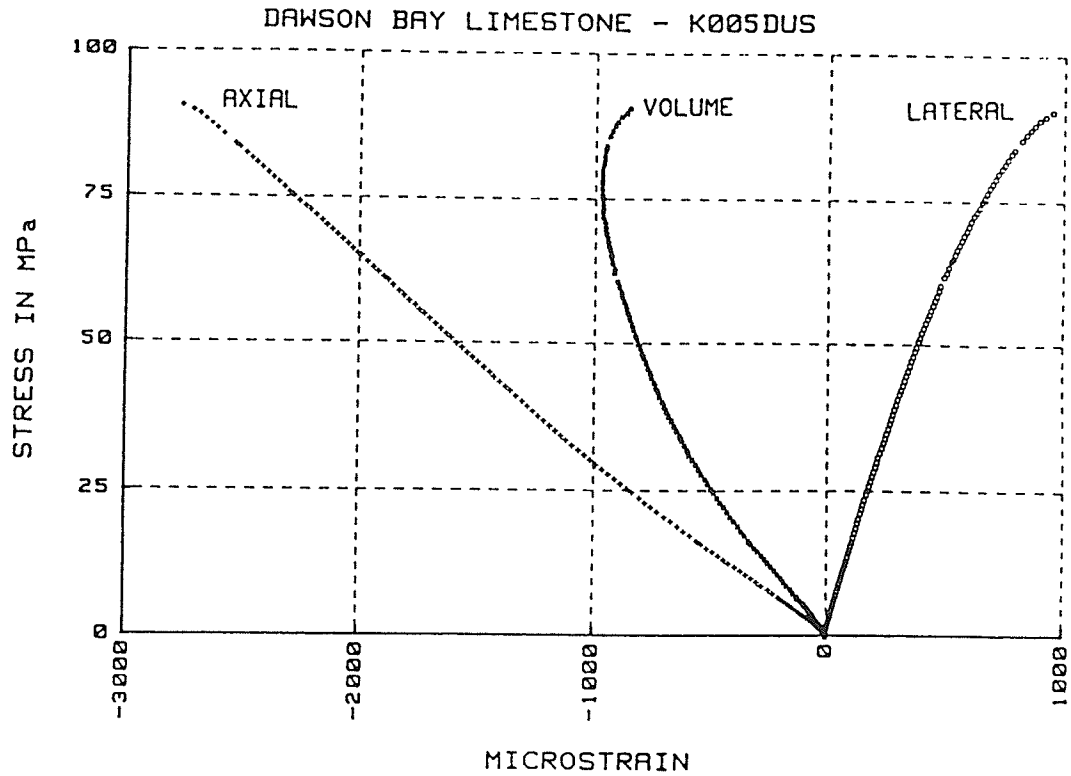

Fig. 4.9 Stress/strain curves for uniaxial compression sample K005DUS

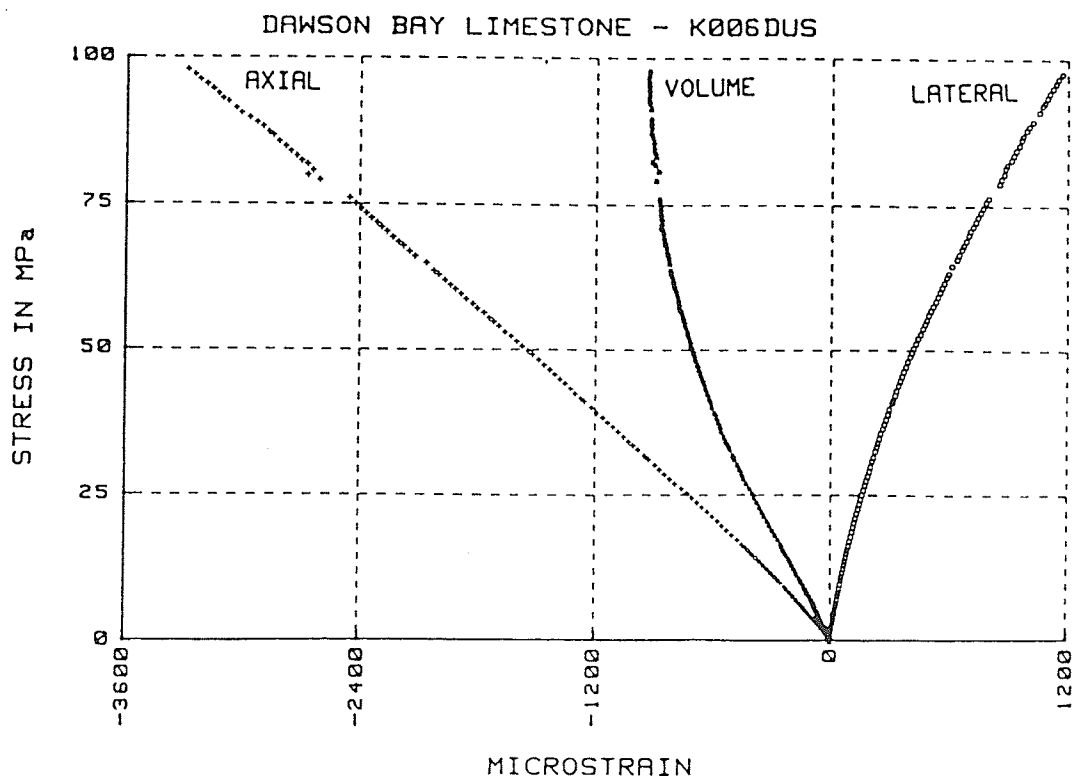

Fig. 4.10 Stress/strain curves for uniaxial compression sample K001DUS

Table 4.2: Compressive deformation moduli results

Sample	Footage (ft)	E MPa	ν
K001DUS	56.0-57.0	26900	0.25
K002DUS	63.0-64.5	22500	0.17
K003DUS	84.2-85.2	49400	0.30
K004DUS	103.0-104.0	46200	0.25
K005DUS	149.0-150.8	29600	0.21
K006DUS	177.6-178.6	29700	0.34

Average Young's modulus of elastisity = 34100 +/- 11000 MPa
Average Poisson's ratio = 0.25 +/- 0.06

4.4 BRAZILIAN TEST RESULTS

Twenty-eight samples were tested in total using representative specimens from the entire core available to us. The footage, diameter, thickness and failure load of each sample are tabulated in Table 4.3. Brazilian tensile strengths are plotted in the form of a histogram in Figure 4.11.

It was observed that tensile failure did not occur at the centre in the 89 mm samples. Instead, the samples failed by spalling on the faces close to the line of application, then in compression (See Figure 4.12). The spalling occurred as a result of the intense stress condition developed at the points of contact between the test specimen and the two flat steel platens. The eight 89 mm samples therefore were not included in calculating the average value of the Brazilian strength and they are not shown in Figure 4.12. It is interesting to note that the calculated tensile stress at the point of failure in compression was within the range of one standard deviation of the tensile strength of the 42 mm samples and was only slightly smaller.

The average Brazilian strength of the 42 mm samples is:

$$\sigma_t = 9.76 +/- 2.68 \text{ MPa.}$$

and the average "Brazilian strength" of the 89mm samples is:

$$\sigma_t = 8.45 +/- 2.07 \text{ MPa.}$$

4.5 TRIAXIAL TEST RESULTS

Forty-five triaxial samples were tested in total with specimens coming from all parts of the available core. The results of these tests are given in Table 4.4. A scatterplot of the axial stress on the sample

(S1) versus the confining stress on the sample (S3) reveals that the results scatter widely but seem to follow two general trends; the grey limestone, which comprises the Burr and much of the Neely members, having a much higher strength than the dark brown highly fossiliferous limestone located at the top of the Neely formation (Fig. 4.13). The data was fit

Table 4.3 : Brazilian tensile strength test data for both sample diameters

Sample	Core Source	Footage (feet)	Diameter (mm)	Thickness (mm)	Load (lbs)	σ_t (MPa)
K001DB	CCP.84-2	136.5-137.5	41.7	25.8	4150	11.26
K002DB	"	"	"	25.5	3780	9.75
K003DB	"	"	"	26.8	3260	8.26
K101DB	"	56.0-58.0	"	23.6	3445	9.91
K102DB	"	63.0-64.5	"	23.7	3950	11.32
K103DB	"	84.2-85.2	"	23.7	3050	8.74
K104DB	"	103.0-104.0	"	23.7	4120	11.83
K105DB	"	149.8-150.8	"	23.2	3800	11.12
K106DB	"	177.6-178.6	"	22.1	4040	12.41
K201DB	"	56.0-57.0	"	23.4	3015	8.54
K202DB	"	61.5-62.0	"	23.1	5120	14.98
K203DB	"	63.0-64.5	"	24.1	2680	7.39
K204DB	"	"	"	26.1	4230	10.94
K205DB	"	84.2-85.2	"	24.5	5050	14.04
K206DB	"	"	"	24.2	3120	8.72
K207DB	"	95.0-96.0	"	25.2	4200	11.27
K208DB	"	103.0-104.0	"	26.0	2010	5.22
K209DB	"	128.0-129.0	"	23.4	2900	8.37
K210DB	"	149.8-150.8	"	24.3	2300	6.16
K211DB	"	177.6-178.6	"	22.3	1650	5.00
K301DB	Lanigan	3246.4	88.6	6.7	1250	5.95
K302DB	"	3264.4	"	10.1	2200	6.95
K303DB	"	3272.3	"	11.1	2505	7.20
K304DB	"	3291.3	"	11.7	2700	7.37
K305DB	"	3304.8	"	9.6	2500	8.31
K306DB	"	"	"	12.1	3610	9.52
K307DB	Bredenbury	2708.0	"	9.0	2805	9.95
K308DB	"	"	"	15.1	5850	12.36

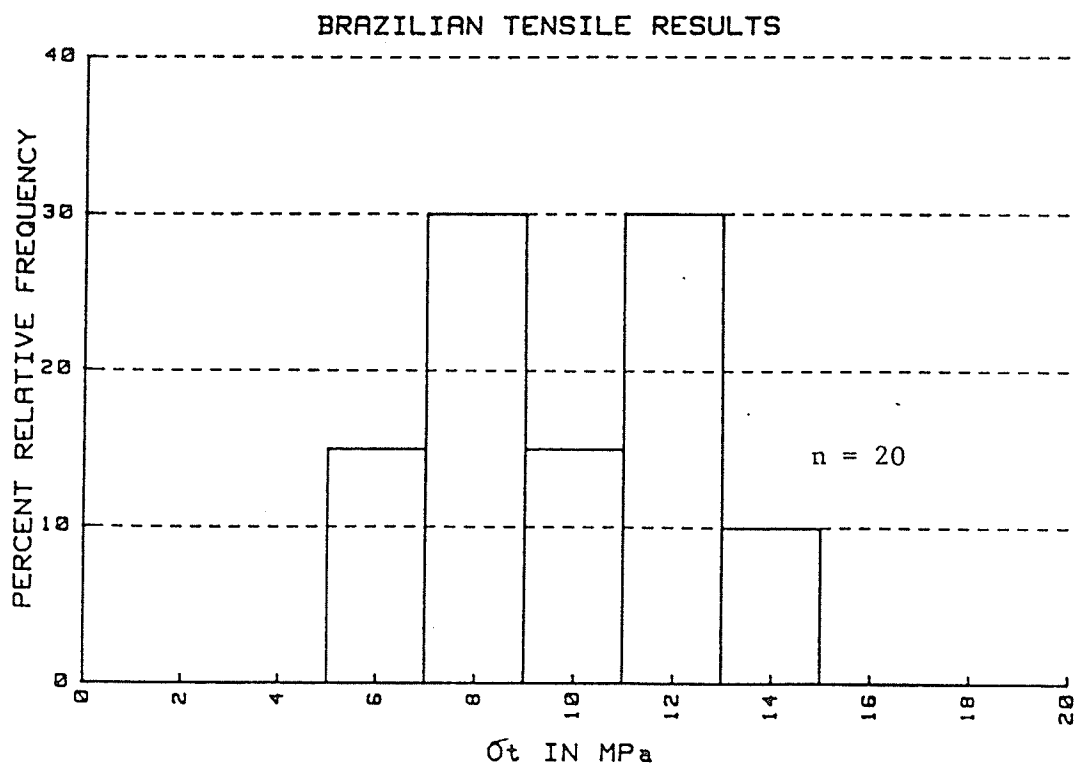

Fig. 4.11 Relative frequency histogram of Brazilian strength tests

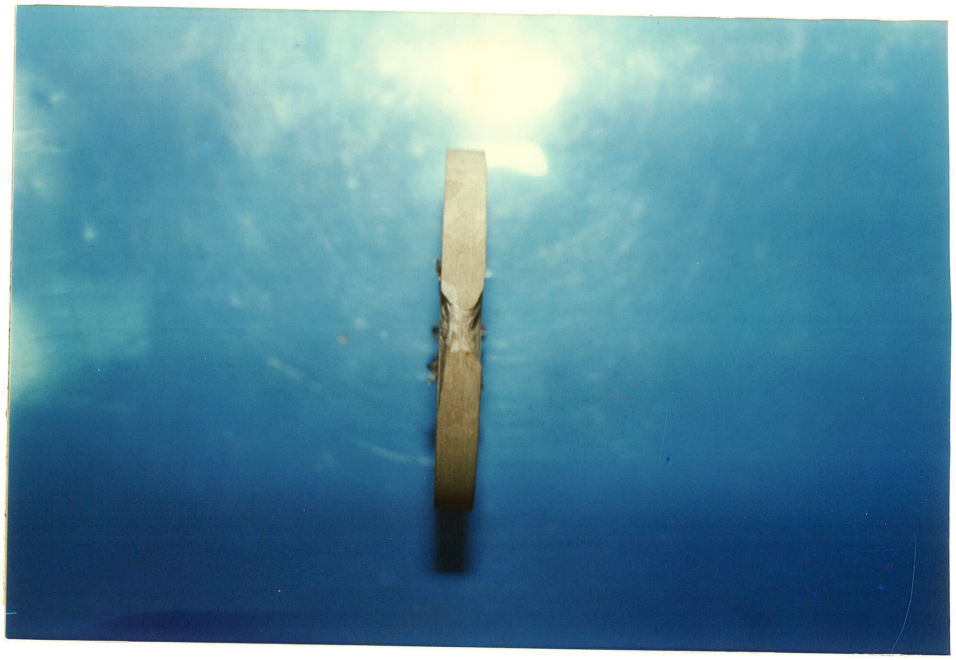

Fig. 4.12 89 mm Brazilian specimen on edge showing spalling failure at point of contact with steel platens

Table 4.4: Triaxial compressive strength test data

Sample	Footage (feet)	h/d	Load (kips)	S3 (MPa)	S1 (MPa)	Fracture Angle *
K001DT	56.0-58.0	1.94	53.44	10	171.40	-
K002DT-1	61.5-62.0	1.97	64.69	15	207.50	62
K002DT-2	61.5-62.0	2.00	76.82	20	246.40	67
K003DT-1	63.0-64.5	2.00	76.65	30	245.80	62
K003DT-2	63.0-64.5	2.00	44.74	40	143.50	60
K004DT-1	65.5-66.5	2.00	59.42	10	190.60	-
K004DT-2	65.6-66.5	2.00	72.87	15	233.70	71
K005DT-1	68.0-69.5	2.00	83.15	20	266.70	62
K005DT-2	68.0-69.5	2.00	74.97	10	246.72	59
K005DT-3	68.0-69.5	2.00	88.04	20	282.68	-
K005DT-4	68.0-69.5	2.00	110.48	40	354.74	60
K006DT-1	79.2-80.2	2.00	94.75	30	303.90	64
K006DT-2	79.2-80.2	2.00	100.03	40	320.80	54
K006DT-3	79.2-80.2	2.00	67.55	10	216.60	63
K007DT	84.2-85.2	2.00	58.10	15	186.30	63
K008DT	89.5-90.5	2.00	98.36	20	315.50	-
K009DT-1	92.0-93.2	2.00	42.37	10	136.40	-
K009DT-2	92.0-93.2	2.00	99.32	20	318.90	56
K009DT-3	92.0-93.2	2.00	86.75	40	278.54	-
K010DT-1	95.0-96.0	2.00	118.40	40	379.70	-
K010DT-2	95.0-96.0	2.00	68.12	10	218.50	-
K011DT-1	101.0-102.0	2.00	72.78	15	233.40	-
K011DT-2	101.0-102.0	2.00	91.41	20	293.20	-
K012DT	103.0-104.0	2.00	77.61	30	248.90	-
K013DT-1	108.2-109.2	2.00	84.38	40	270.60	-
K013DT-2	108.2-109.2	2.00	55.11	10	176.70	60
K013DT-3	108.2-109.2	2.00	74.27	15	138.20	65
K014DT-1	112.8-114.0	2.00	62.41	20	200.20	77
K014DT-2	112.8-114.0	2.00	25.31	0	81.20	-
K015DT-1	121.0-122.0	2.00	87.81	40	281.60	65
K015DT-2	121.0-122.0	2.00	55.03	10	176.50	-
K016DT-1	143.0-144.2	2.00	63.10	10	202.61	57
K016DT-2	143.0-144.2	2.00	90.35	20	290.10	67
K016DT-3	143.0-144.2	2.00	84.29	40	270.64	50
K017DT-1	147.2-148.2	2.00	62.85	15	201.60	73
K017DT-2	147.2-148.2	2.00	80.69	20	258.80	78
K018DT	149.8-150.8	2.00	27.42	0	87.90	62
K019DT-1	155.8-156.8	2.00	52.91	40	169.70	-
K019DT-2	155.8-156.8	2.00	25.67	10	82.30	65
K020DT-1	157.8-158.8	2.00	38.32	15	122.90	-
K020DT-2	157.8-158.8	2.00	43.69	20	140.10	56
K020DT-3	157.8-158.8	2.00	12.48	0	40.00	63
K021DT	177.6-178.6	2.00	17.93	0	57.50	72
K022DT	180.8-181.5	2.00	35.69	40	114.50	-
K023DT-1	1-RED-BED	2.00	34.98	10	112.32	57
K023DT-2	1-RED-BED	2.00	39.20	20	125.87	52

* Fracture angle measured from the horizontal

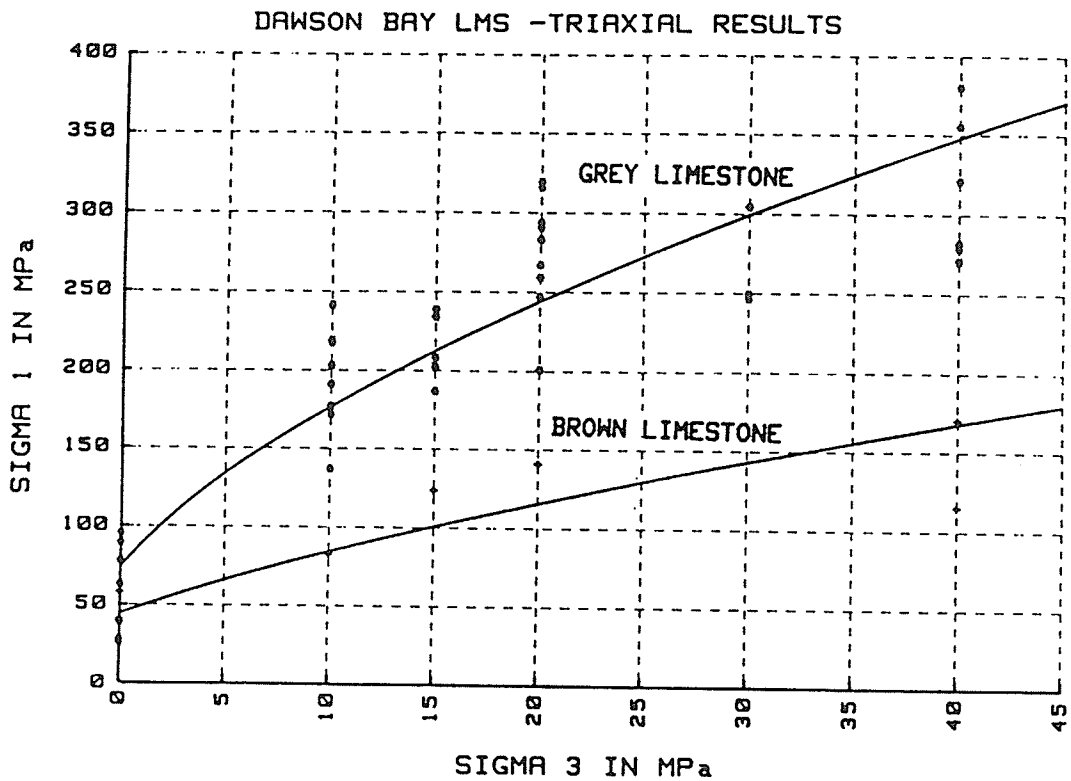

Fig. 4.13: Scatterplot of axial stress (Sigma 1) versus confining stress (Sigma 3) showing two general trends (* denotes the grey limestone data and + denotes the brown limestone data)

to several models, but only the empirical relationship suggested by Hoek and Brown (1980) is shown as the solid lines in Figure 4.13. The empirical relationship given by Hoek and Brown follows the following form:

$$\sigma_1 = \sigma_3 + \sqrt{(m * \sigma_c * \sigma_3 + \sigma_c^2)} \quad (4.5)$$

where: σ_1 = the major principal stress at failure

σ_3 = the minor principal stress applied to the specimen, in this case the confining pressure

σ_c = the uniaxial compressive strength of the intact rock material in the specimen

m, s = constants which depend on the properties of the rock

The constants m and s were derived from a series of equations given by Hoek and Brown (1980), and are included in the following triaxial strength equations for the grey and brown limestone respectively:

$$\sigma_1 = \sigma_3 + \sqrt{(25.96 * 80.78 * \sigma_3 + 80.78^2)} \quad (4.6)$$

$$\sigma_1 = \sigma_3 + \sqrt{(8.14 * 44.14 * \sigma_3 + 44.14^2)} \quad (4.7)$$

4.6 SHEAR TEST RESULTS

Friction is defined through Amonton's law, stating that the maximum amount of frictional resistance (F) in a plane of sliding is directly proportional to the normal load on the plane through a constant of proportionality known as the coefficient of friction (μ). The coefficient of friction is a property of the material, and is independent of the size of the apparent contact area.

Six direct shear tests were conducted on a single Dawson Bay Limestone sample using the progressively wearing surface. The

results from these tests are best described by the use of an angle of friction, which is calculated by taking the arctangent of the quotient obtained by dividing the shear stress (τ) by the normal stress (N) at the point of the first slippage on the worn surface of the sliding block.

$$\phi = \arctan\left(\frac{\tau}{N}\right) \tag{4.8}$$

The results from all the direct shear tests are presented in Table 4.5. The mean friction angle from these tests is:

$$\phi = 33.42 +/- 2.35 \quad \text{(deg.)}$$

Table 4.5: Direct shear test results

Test	Rate of Shear Loading (kN/s)	Duration of Normal Stress Before Shearing (s)	Angle of Friction (ϕ) (degrees)
K001DD	0 0055	39	33.33
K002DD	0.0133	0	31.75
K003DD	0.0310	20	35.61
K004DD	0.2250	0	33.50
K005DD	0.1820	101	29.99
K006DD	0.0470	0	36.29

(ϕ is the friction angle taken at the first slip of the limestone surfaces)

4.7 STATIC FATIGUE TESTING

4.7.1 Theoretical aspects of static fatigue testing

Intact rock seems to be little different from most industrial products or other objects with regard to having a limited life expectancy. The determination of the life of a rock under stress is not easy, however, because of the nonhomogeneous nature of rock. The life of a Dawson Bay Limestone sample under constant sustained loading, for example, can range from one second to over a month.

Because of the wide range of time to failure measurements observed in the testing, a probablistic approach was used in data interpretation. Lajtai (1986) attributed the wide range of time to fracture measurements in rock to variations in instantaneous strength in the rock specimens. At the same static fatigue load, a weaker specimen is subjected to a much higher relative stress level (static fatigue load divided by the instantaneous, compressive, strength of the specimen) than a stronger specimen. The higher relative stress level results in a shorter life of the sample.

Snowden developed a technique where the Weibull statistical distribution is utilized in modelling the distribution of both the instantaneous failure strength and the failure time at constant stress (Snowden, 1977). Using the two parameter form of the Weibull distribution, the cumulative probability of failure (P) of a specimen of volume (v) subjected to a stress (σ) for a time (t) can be expressed as:

$$P = 1 - \exp\left[-\left(\frac{\sigma}{\sigma_o} \right)^m \left(\frac{v}{v_o} \right) \left(\frac{t}{t_o} \right)^w \right] \qquad (4.9)$$

where: σo, vo, to, m and w are Weibull constants. It can be concluded by examining equation 4.9 that an increase of either stress, the volume,

or the loading time will result in an increase in the probability of failure.

4.7.2 Modelling of static fatigue data

The Weibull distribution was used to analyze both the uniaxial compressive strength tests and the time to failure tests. Seventeen samples were tested in each set. Each set was randomly drawn from a larger group of specimens.

Since uniaxial compression testing is conducted in a constant time and the volume of each specimen was the same (38300 mm^3), the Weibull theory used to describe the strength distribution was simplified to :

$$P = 1 - \exp\,[-Z\,\sigma_L^m] \qquad (4.10)$$

where Z is a constant that combines all the non varying parameters and other constants in equation 4.9, and σ_L is the stress level calculated by dividing the static fatigue load with the strength of the specimen and is expressed in percentage form.

Similarily, the distribution of the time to failure experiments was analysed using the same form of this probability function for constant stress (static load) and constant volume conditions. The form of the function became:

$$P(t) = 1 - \exp\,[\,-Y\,t^w\,] \qquad (4.11)$$

where Y is the constant that combines all the non varying parameters and constants in equation 4.9 (t is time to failure in seconds). The four constants Z, m, Y and w were determined from the two test series. In particular Z and m were calculated from the 17 uniaxial compression tests (Table 4.6) and Y and w were calculated from the 17 static fatigue tests

(Table 4.7).

The uniaxial testing was performed on samples representing the Dawson Bay limestone in its entirety. The tests were conducted at a very fast loading rate in a perfectly dry environment. This testing was done to obtain results for the instantaneous strength of the Dawson Bay limestone. Table 4.6 shows the results of the tests, ranking the sample strengths from lowest to highest. The mean compressive strength of the 29 mm diameter samples was:

$$\sigma_c = 115 \text{ MPa}$$

The static fatigue test samples were subjected to a constant stress of 60 MPa, or about 52 % of the average uniaxial compressive strength of the samples. During the test, the samples were submerged in tap water. The time measurements yielded a distribution of failure times from instantaneous to longer than a month. Three samples, ranked 15, 16, and 17, did not fail under the static loading. Table 4.7 shows the time to failure results ranked in order to longest time to failure. The cumulative probability associated with each rank can be approximated by equation 4.12,

$$P=i/(N+1) \tag{4.12}$$

Table 4.6: Dry compressive strength of Dawson Bay Limestone specimens used in the static fatigue study

Rank	Strength (MPa)
1	59
2	66
3	67
4	77
5	79
6	89
7	91
8	105
9	106
10	106
11	112
12	118
13	165
14	171
15	174
16	174
17	191

$n = 17$

$\overline{x} = 115$ MPa

$s = 43.7$ MPa

Table 4.7: Time to failure results for Dawson Bay Limestone at a static fatigue stress of 60 MPa. Specimens 15, 16, and 17 did not fail over a period of: 4 days, 31 days, and 35 days respectively. The stress level is obtained by dividing the static fatigue load (60 MPa) with the strength of the specimen having the same rank in Table 4.6 and the result expressed is a percentage form.

RANK	TTF (s)	STRESS LEVEL (%)	CUMULATIVE PROBABILITY
1	1	102	0.05556
2	1	91	0.11111
3	1	90	0.16667
4	2	78	0.22222
5	4	76	0.27778
6	8	67	0.33333
7	8	66	0.38889
8	10	57	0.44444
9	12	57	0.50000
10	16	57	0.55555
11	62	54	0.61111
12	240	51	0.66667
13	295	36	0.72222
14	2460	35	0.77778
15	no break	34	0.83333
16	no break	34	0.88889
17	no break	31	0.94444

where i is the rank and N is the total number of tests. The constants Y, Z, w, and m of the Weibull distribution were then evaluated by linearizing equations 4.10 and 4.11 and then plotting lnln [1/(1-P)] against ln (σ) and against ln (t) for each determination. These plots should result in straight line curves where:

$$\ln\ln (1/(1-P(\sigma))) = \ln (Z) + m \ln (\sigma) \qquad (4.13)$$

$$\ln\ln (1/(1-P(t))) = \ln (Y) + w \ln (t) \qquad (4.14)$$

The constants m and w are the slopes of the straight lines and ln (Z) and ln (Y) are the intercepts. The results obtained from this experimental suite yielded the following relationships:

$$\ln\ln (1/(1-P(\sigma))) = \ln (-13.205) + 2.714 \times \ln (\sigma) \qquad (4.15)$$

$$\ln\ln (1/(1-P(t))) = \ln (-1.351) + 0.271 \times \ln (t) \qquad (4.16)$$

Figures 4.14 and 4.15 show these relationships. Figures 4.16 and 4.17 show the non-linearized Weibull fit to the cumulative probability versus strength data.

On the assumption that the weakest specimen failed first and the strongest last, ie. a specimen ranked i in the strength distribution has the failure time at the same rank i, a static fatigue curve can be constructed following the technique described in Lajtai et al. (1986) giving the relationship between stress level (σ_L) and time (t):

$$\mathrm{Ln}\ (\sigma_L) = -4.370 + (\mathrm{Ln}\ 60 - .1 \times \mathrm{Ln}\ (t))$$

$$\mathrm{Ln}\ (t) = -43.8 + 10 \times \mathrm{Ln}\ (60/\sigma_L)$$

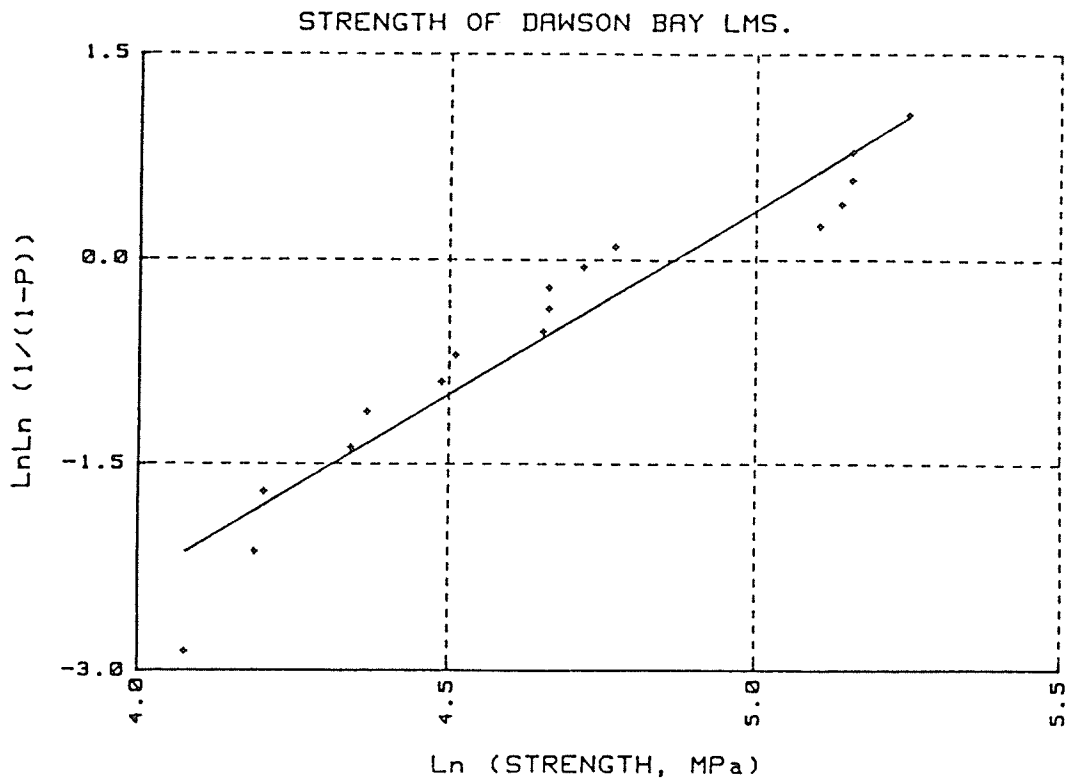

Fig. 4.14 Linear regression line of strength of Dawson Bay Limestone with the Weibull distribution fitted to it

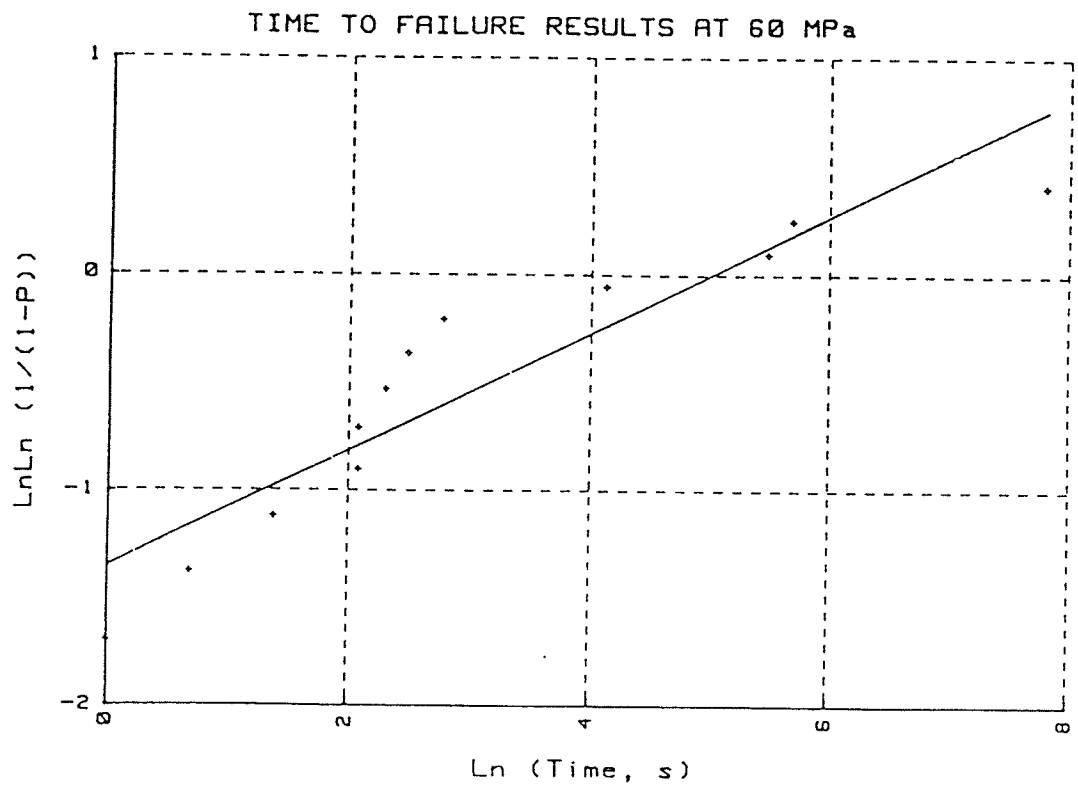

Fig. 4.15 Linear regression line of time to failure data for Dawson Bay Limestone (load = 60 MPa) with the Weibull distribution fitted to it

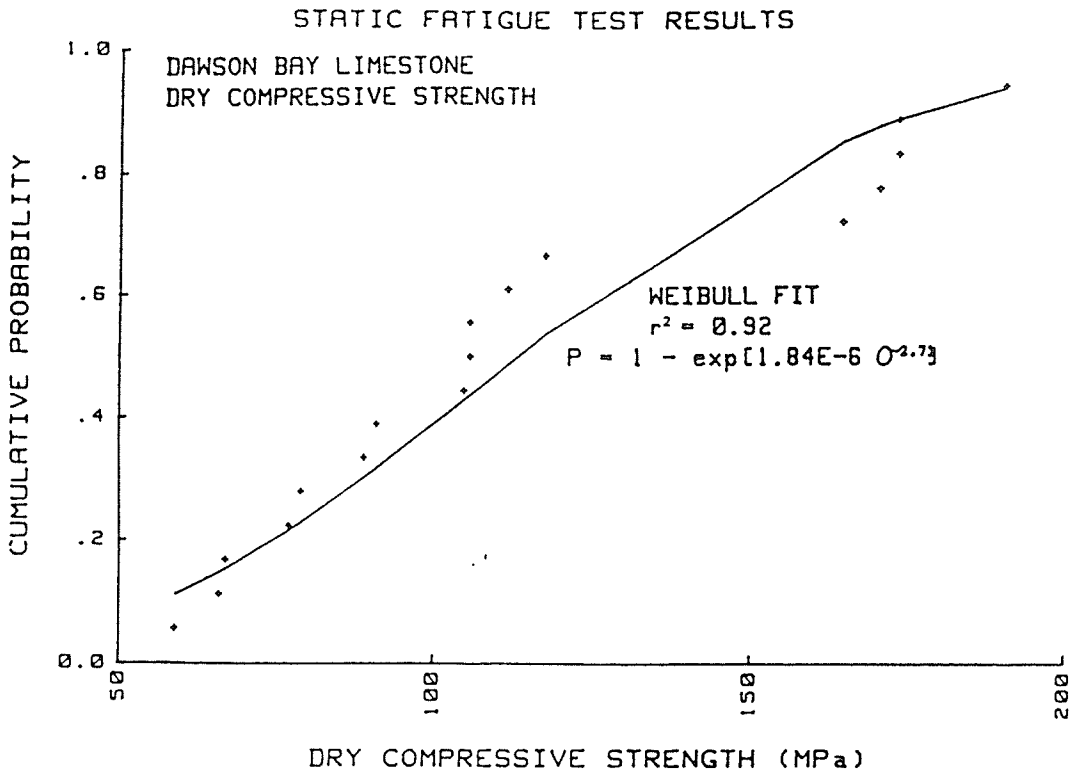

Fig. 4.16 Weibull distribution plotted with strength data for Dawson Bay Limestone (N=17)

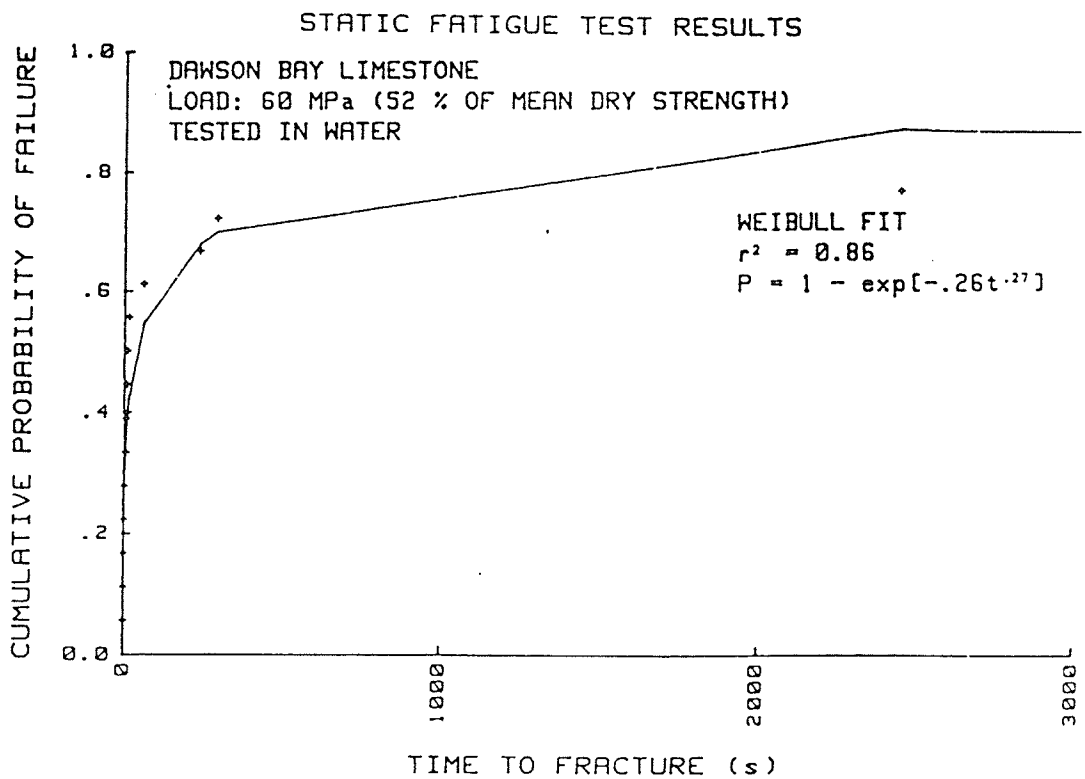

Fig. 4.17 Weibull distribution plotted with the time to failure data for the Dawson Bay Limestone at a constant stress of 60 MPa

4.7.3 Static fatigue limit

In addition to the stress/time relationships developed in the previous section, a static fatigue curve (stress level against time) can also be constructed without reference to the Weibull distribution. Schmidtke (1986), and Lajtai and Schmidtke (1986) observed in the course of their work with static fatigue experimentation on granite, anorthosite and Tyndal limestone, that the slope of the static fatigue curve decreases with decreasing static fatigue stress. This suggests that a static fatigue limit, i.e. a stress level below which no failure occurs at anytime, exists for most rock types.

This limiting feature for Dawson Bay Limestone is shown in Figure 4.18 where the stress level is plotted against time (s). In order to model the data, a Ln (time), Ln (stress level) plot (Fig. 4.19) was constructed after Lajtai (1986) and a standard non linear regression was performed using an exponential function of the form :

$$Y = A \exp (B x) + C \qquad (4.18)$$

The equation that best models the relationship is shown by the solid line in Figure 7.19 and is given mathematically by:

$$\mathrm{Ln}\ (\sigma_L) = 1.63 \exp (-0.11 * t) + 2.68 \qquad (4.19)$$

For very long failure times, the exponential term becomes zero. The C term then, becomes the static fatigue limit. For the case of Dawson Bay Limestone, the static fatigue limit which will not cause failure is $\mathrm{Ln}\ (\sigma_L) = 2.86$. Expressed as a percentage of the stress level the value is 17.5% or 20 MPa. In other words, saturated Dawson Bay limestone will never fracture if it is subjected to a uniaxial static load less than 20 MPa.

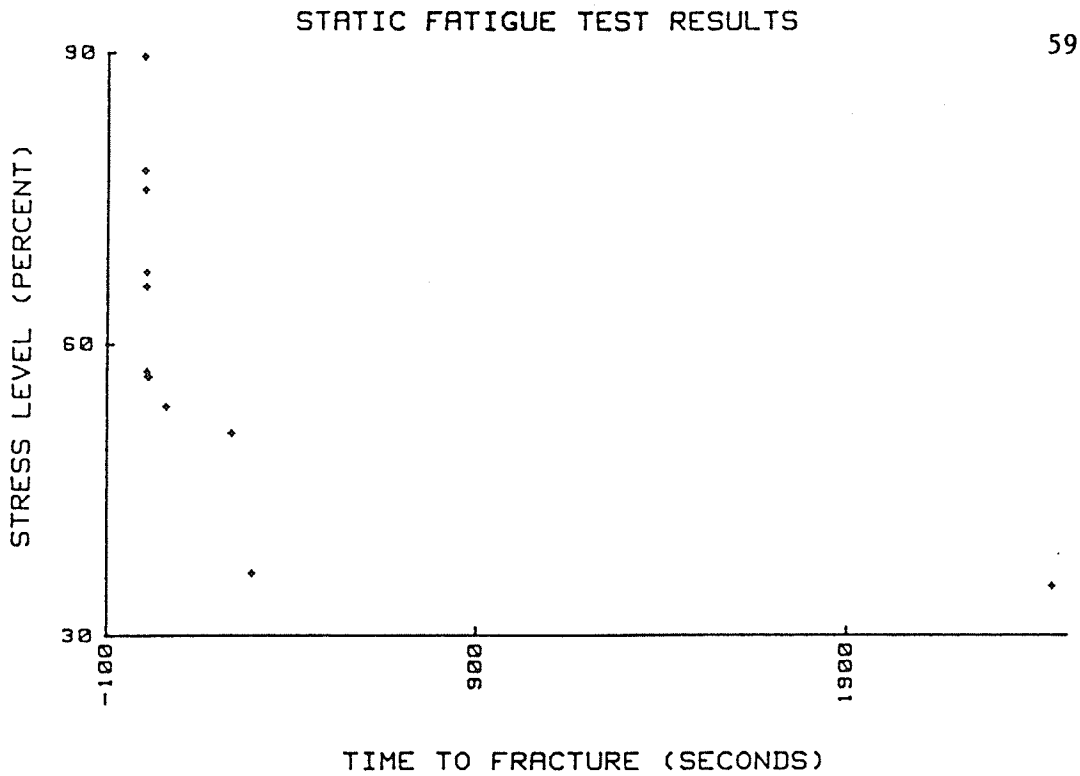

Fig. 4.18 Time to failure results showing curve becoming asymtotic at low stress level

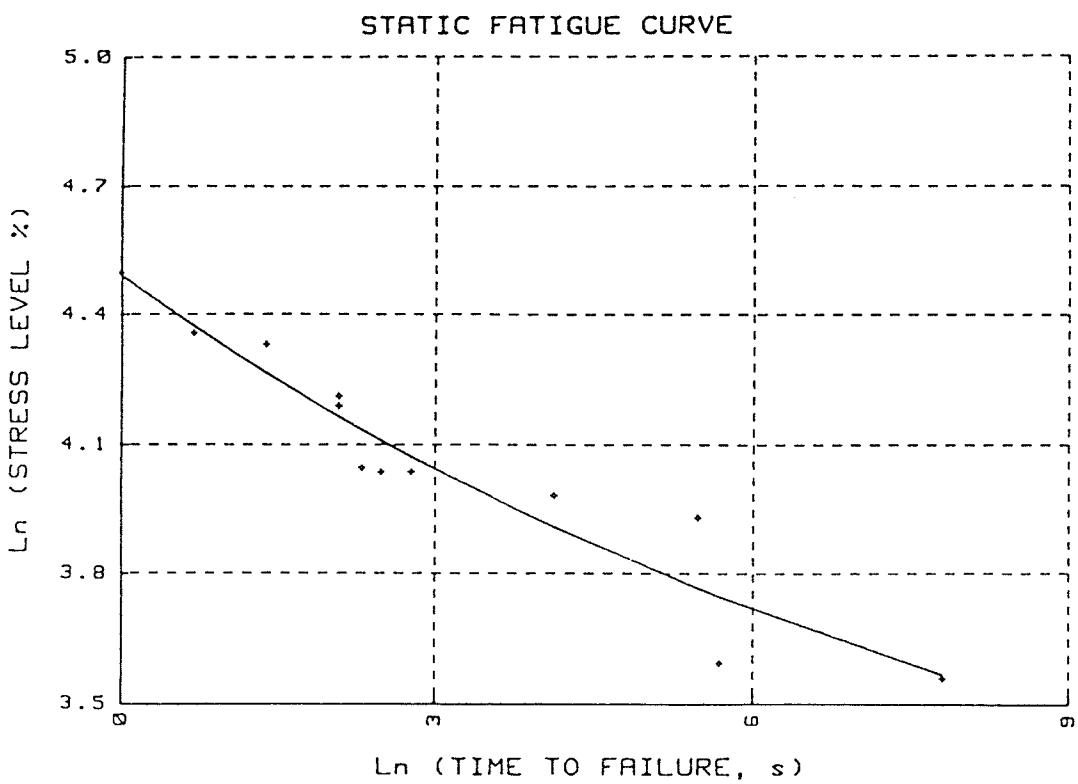

Fig. 4.19 Static fatigue curve for Dawson Bay limestone showing limiting trend for lower stress level

CHAPTER 5.0

INDIRECT TENSILE MODULI EXPERIMENTATION

The same problems that exist in determining the uniaxial tensile strength of brittle materials are inherent in finding the uniaxial tensile deformation moduli of brittle materials, since the test set up is virtually the same. An experimental technique was therefore developed using strain gauged Brazilian samples to determine the two tensile moduli E_t and ν_t.

5.1 THEORY

Theoretically, the derivation of the tensile deformation moduli can be done using Hoek's law. Figure 5.1 shows a line loaded Brazilian test in section and the forces acting on an element in the centre. Both compressive and tensile stresses will act on the element causing strains in directions parallel to both of the principal stresses. An increase in the major principal stress, will result in shortening of the element in the σ_1 direction. A decrease of the minor principal stress (ie. an increase in the tensile stress) will result in an lengthening of the element in the σ_3 direction. For a linearly elastic, homogeneous material, these strains can be determined from the elastic moduli of the material and at a certain stress state by Hoek's law. The strains in the principal stress directions are given by:

$$\varepsilon_c = \sigma_1 / E_c + \nu_t \sigma_3 / E_t \qquad (5.1)$$

$$\varepsilon_t = \sigma_3 / E_t + \nu_c \sigma_1 / E_c \qquad (5.2)$$

where all the parameters (stress, strain, moduli) are given in absolute

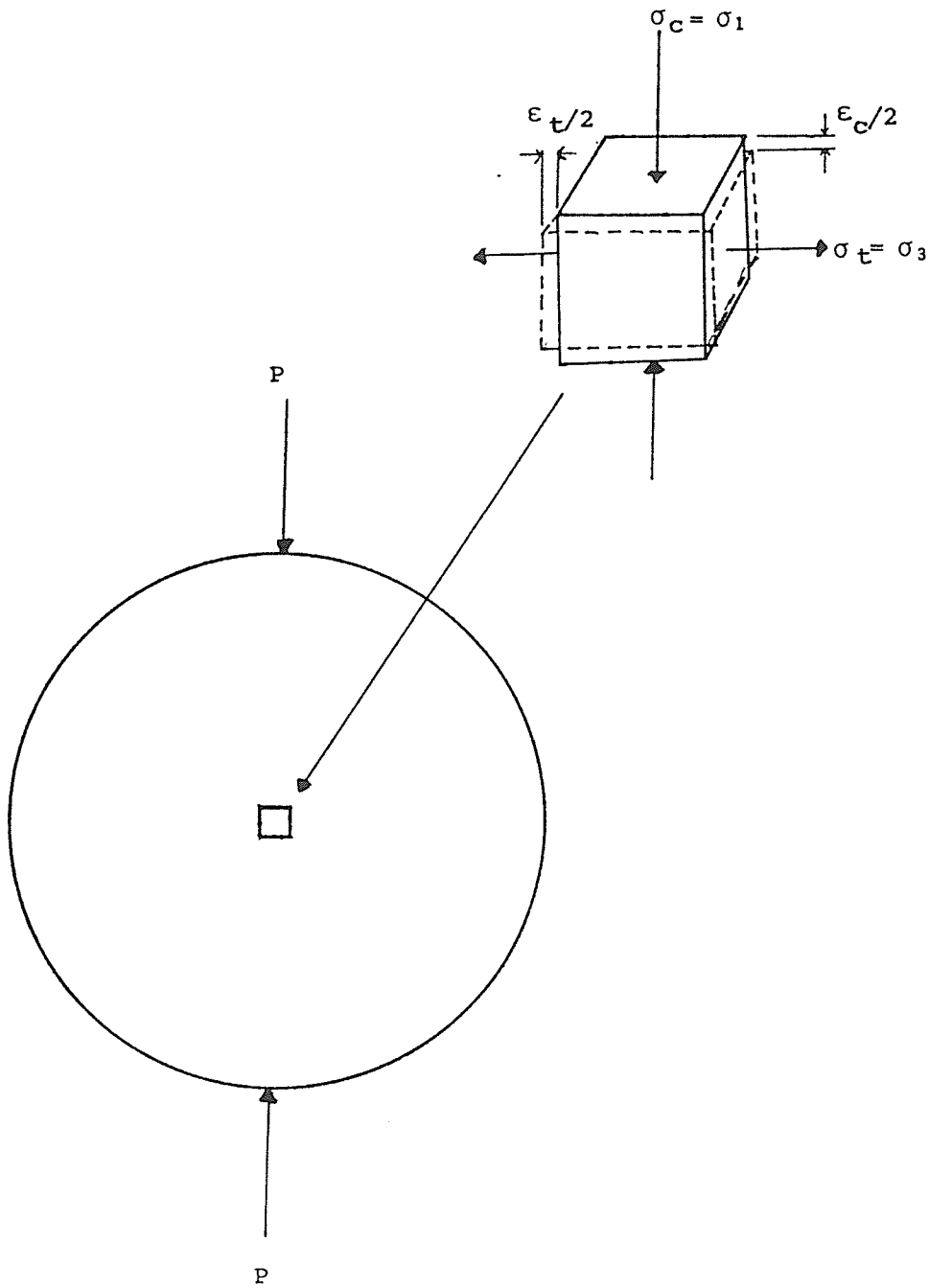

Fig. 5.1 Stresses and strains acting on an element at the center of a theoretical Brazilian test specimen

values. ε_c is the compressive principal strain and ε_t is the tensile principal strain and the subscripts t and c identify the constants for tension and compression respectively. Simplifying these equations for E_t and ν_t we get:

$$E_t = \sigma_3 / (\varepsilon_t - \nu_c \sigma_1 / E_c) \tag{5.3}$$

$$\nu_t = (\varepsilon_c - \sigma_1 / E_c) E_t / \sigma_3 \tag{5.4}$$

We can obtain E_c and ν_c from uniaxial compressive testing and ε_c and ε_t from a strain gauged Brazilian test. σ_1 and σ_3 can be derived analytically from the Brazilian test:

$$\sigma_3 = P/(\pi R t) \tag{5.5}$$

$$\sigma_1 = -3P/(\pi R t) \tag{5.6}$$

where: P = point load applied to disc
t = disc thickness
R = radius of disc

5.2 COMPRESSIVE MODULI

The first testing done was to determine the compressive moduli parallel to the bedding plane and to examine if the moduli were in fact similar in directions both parallel and perpendicular to the bedding plane. To investigate this, two 31 mm samples were cored parallel to the bedding plane at two different footages from 89 mm core. The samples were then strain gauged and tested in uniaxial compression with the results given in Table 5.1. The compressive moduli perpendicular to the bedding plane is taken using sample descriptions and results from Dunn (1982). Table 5.1 shows that the elastic moduli perpendicular to the bedding plane is not much different than the moduli parallel to the bedding plane. From this point onward then, it is assumed that the compressive moduli in both directions are approximately equal (ie. the

rock is isotropic). This assumption allows us to use moduli results from previous perpendicular compression tests to examine the tensile moduli parallel to the bedding plane.

5.3 INDIRECT TENSILE MODULI RESULTS

Seventeen strain-gauged Brazilian tests were conducted in total using two different diameter specimens: 42 mm and 89 mm. Two types of strain gauges were also used, 5 mm long standard SHOWA strain gauges and 60 degree strain rosettes composed of strain gauges 2 mm in length. The theoretical stress distribution throughout the disk along the vertical (parallel to loading) and horizontal diameters is given by Figure 5.2. At the centre of the disk, the tangential stress on the X axis is equal to the radial stress on the Y axis and the radial stress on a point on the X axis is equal to the tangential stress acting on a point on the Y axis. The tensile stress (σ_3) undergoes little change along the Y axis and the compressive stress (σ_1) remains reasonably constant at the centre.

The test specimens were divided into four groups according to the chronological order of testing: K000DB, K100DB, K200DB, and the K300DB series. Results that were obtained from K000DB and K100DB series were highly questionable yielding unreasonably high Young's Modulus of Elasticity and some negative Poisson's ratios. It was concluded that these results were due to either improper positioning of the strain gauges or that the gauges were too large for the 42 mm size disc. This problem was corrected for the K200DB and the K300DB series by taking greater care in placing the gauges on the K200DB samples and by using

Table 5.1: Compressive moduli parallel and perpendicular to the bedding plane of the Dawson Bay Limestone

Sample	Footage (m)	E (par) (MPa)	ν (par)	E (per) (MPa)	ν (per)
K302DCS	995	39000	0.289	50300	0.267
K306DCS	1007	41300	0.246	42100	0.269

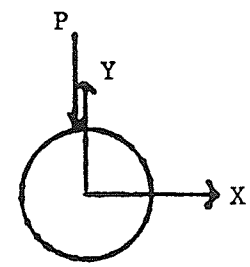

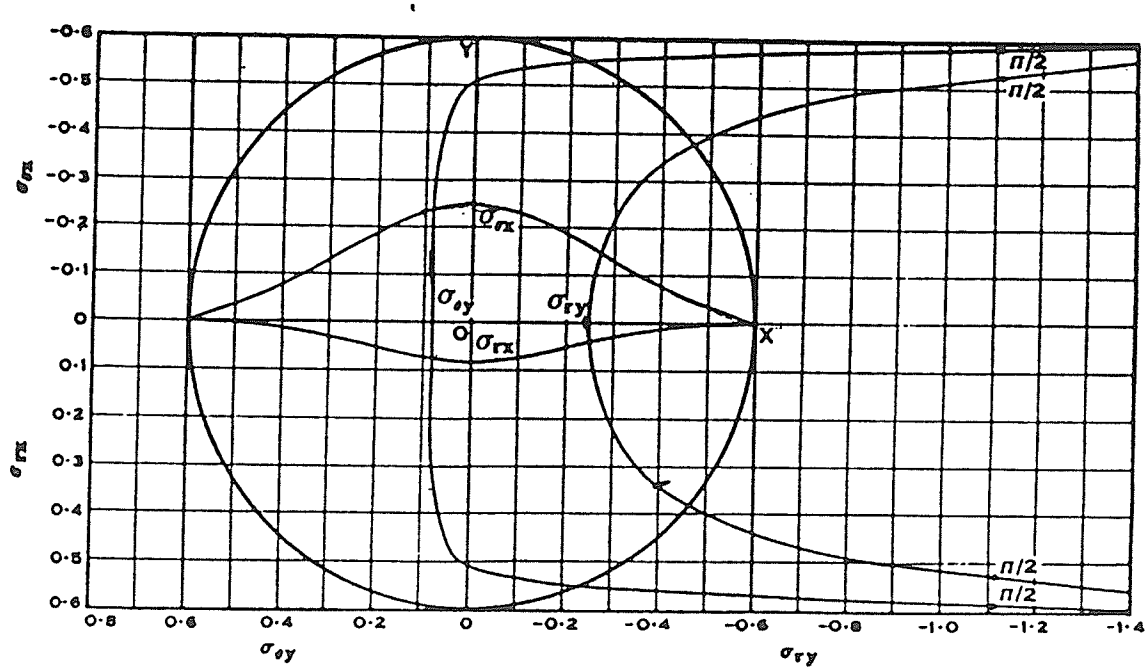

Fig. 5.2 Theoretical stress distribution along the vertical and horizontal dismeters of a Brazilian test specimen (Hondros, 1959)

smaller gauges and the larger K300DB samples. Testing on the K200DB series was performed on 42 mm diameter disks cut from the Central Canada potash mine core with a diameter to thickness ratio of 1.75:1. Compressive results used in the calculations were obtained from compression tests conducted perpendicular to the plane of tensile testing. As shown earlier, these should not be much different from the modulus in the bedding direction.

Testing on the K300DB series was performed on 88.6 mm well core drilled at an angle of 90 degrees to the horizontal with a diameter to thickness ratio of about 9:1. Compressive results used in the calculations were determined from uniaxial compressive testing parallel to the plane of tensile testing on specimens from the same core. Indirect compressive moduli were also computed (from the Brazilian test) to see how they would compare to moduli from compression tests. This was done using the equations by Hondros (1959):

$$\nu = -(3\varepsilon_t + \varepsilon_c)/(3\varepsilon_c + \varepsilon_t) \qquad (5.5)$$

$$E = 2P\ (1 - \nu^2)/(\pi Dt\ (\ \varepsilon_c + \nu\varepsilon_t)) \qquad (5.6)$$

5.3.1 Indirect tensile modulate results - K200DB Series

Eight samples in total were analyzed from the K200DB series at both high and low stress ranges because of the non linear nature of the the Brazilian stress/strain curve (See Figure 5.3). Low stress was defined as a compressive stress of 10 MPa and high stress was defined as a compressive stress near 20 MPa. The compressive moduli were taken as the secant moduli at these two stress levels from the compressive tests. The results of the K200DB test series are given in Table 5.2 and 5.3.

The mean indirect tensile moduli values are compared in Table 5.4. Table 5.4 shows that the value for E_t decreases at the higher stress level. ν_t, however, increases when comparing the high to the low stress levels. The average values for the Young's modulus in tension and Poisson's ratio in tension from these experiments are 26500 and 0.495 respectively. The Young's modulus in tension is approximately 34% less than that in compression. Poisson's ratio in tension is about 127% larger than Poisson's ratio in compression.

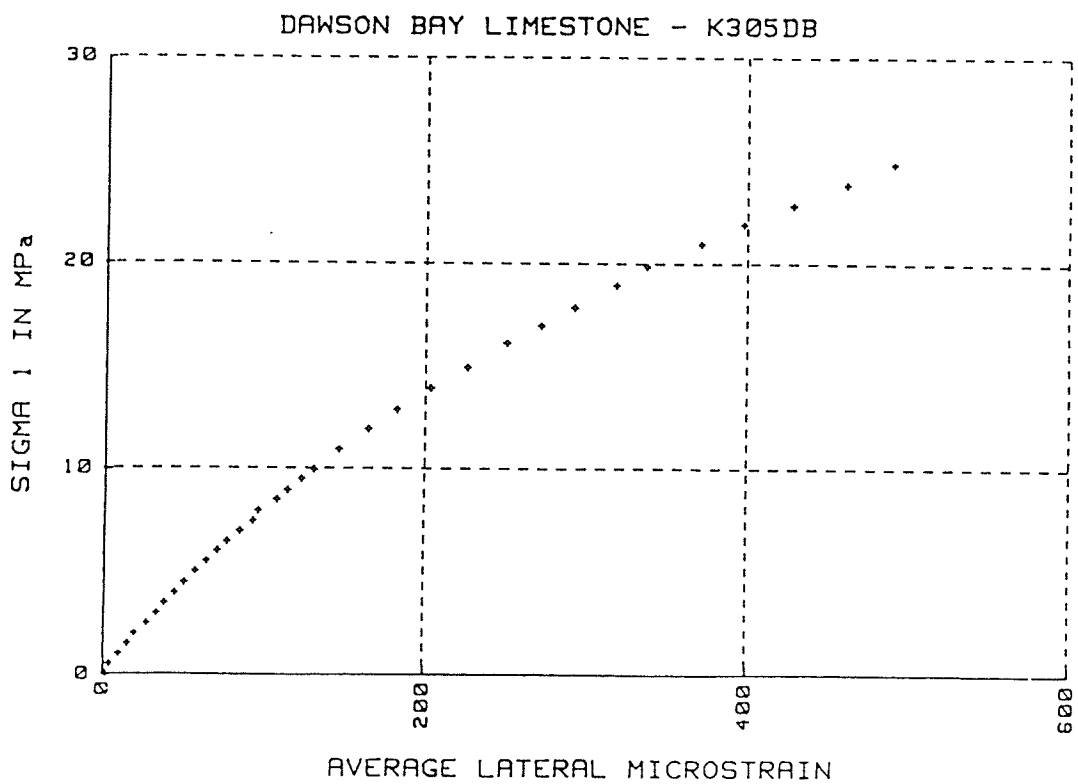

Fig. 5.3 Stress/strain curve for typical Brazilian test

Table 5.2: K200DB test data at low stress level (10 MPa)

Sample	νc	Ec (MPa)	σ_1 (MPa)	ε_a	ε_l	Et (MPa)	νt	E_i (MPa)	ν_i
K201DB	0.235	51100	10.416	305.5	139.0	38100	1.120	35700	0.143
K203DB	0.177	30500	10.092	388.0	199.0	24000	0.407	28000	0.217
K204DB	0.177	30500	10.166	333.0	143.0	40300	-0.040	31700	0.112
K205DB	0.191	49400	10.138	183.0	105.5	51000	-0.335	61000	0.301
K206DB	0.191	49400	9.972	249.0	128.5	37000	0.524	43000	0.221
K208DB	0.300	53200	10.127	335.5	223.5	20300	0.872	34500	0.428
K210DB	0.201	29900	10.452	439.5	358.0	12100	0.313	29000	0.661
K211DB	0.217	38200	9.817	504.5	423.0	8900	0.674	24000	0.701

Table 5.3: K200DB test data at high stress level (20 MPa)

Sample	νc	Ec (MPa)	σ_1 (MPa)	ε_a	ε_l	Et (MPa)	νt	E_i (MPa)	ν_i
K201DB	0.270	42100	20.832	953.0	462.0	21100	1.400	23200	0.181
K203DB	0.180	26600	20.226	1059.5	723.0	11500	0.510	22000	0.452
K204DB	0.180	26600	20.176	766.0	353.0	31000	0.035	27700	0.151
K205DB	0.236	50300	20.027	398.0	225.5	50800	-0.001	55100	0.288
K206DB	0.236	50300	20.280	616.5	352.0	26300	0.831	36000	0.293
K208DB	0.279	49600	13.165	473.5	331.0	17100	0.810	32200	0.477
K210DB	0.203	28800	16.884	718.5	693.0	9800	0.230	30800	0.930

Table 5.4: Mean indirect tensile modulae for high and low stresses (200DB series)

STRESS LEVEL	E (MPa)	νc	Et (MPa)	νt	E_i (MPa)	ν_i
Low (10 MPa)	41500 (10300)	.211 (0.041)	29000 (14800)	.446 (.447)	35900 (11700)	.348 (.227)
High (20 MPa)	38700 (10700)	.225 (.037)	23900 (14100)	.544 (.509)	32400 (11100)	.396 (.266)
Average	40100	.218	26500	.495	34100	.372

5.3.2 Indirect tensile moduli results - K300DB Series

This testing series was conducted in order to determine if increasing the diameter (D) and the diameter to thickness (t) ratio had any substantial effect on the indirect tensile results. Two different types of strain gauges were used: a standard strain gauge and a strain rosette composed of three strain gauges. The two types of strain gauges were positioned as shown in Figures 5.4 and 5.5 on each side of the sample. Both types of gauges gave the same results as shown in Figure 5.6 and 5.7.

Three 88.6 mm diameter samples were analyzed using compressive moduli values obtained parallel to the tensile testing plane. Samples K305DB and K306DB were cut from the same core segment. The results from these tests for both high and low stress are given in Tables 5.5 and 5.6. The average tensile deformation moduli for the three samples are given in Table 5.7.

It is evident from the 300 test series, that the average Young's Modulus in tension is about 37% lower that the average Young's modulus in compression. The average Poisson's ratio in tension is about twice as much, or 205% the value of Poisson's ratio in tension.

5.3.3 Comparison of results from the different size Brazilian samples

The average values for the Young's modulus in tension and the Poisson's ratio in tension from the 42mm diameter experiments (K200DB series) are 26500 MPa and 0.495 respectively. These values result in a Poisson's ratio in tension which is 127% higher than ν_c and a Young's modulus in tension 34% lower than E_c . The results from the 89mm

specimens (K300DB series) reveal that the Poisson's ratio in tension is about 50% higher than ν_c, and E_t is about 37% lower than the Young's modulus in compression.

Together, the results indicate that the determination of E_t is relatively insensitive to the diameter of the specimen used. However, it is obvious that a change of sample diameter affects the values for ν_t. A possible explanation for this is that the 89mm disks were much thinner (diameter to thickness ratio of 9:1) than the 42mm disks (diameter to thickness ratio of 2:1), and the stress regime within the 89mm sample, based on the plane stress condition, was therefore more closely predicted by the analytical formulae.

5.3.4 Determination of compressive deformation moduli by indirect means

Determination of the compressive deformation moduli E_i (Young's modulus in compression) and ν_i (Poisson's ratio in compression) was performed indirectly using the stress strain data from the strain gauged Brazilian tests, and theory and equations (5.5) & (5.6) by Hondros (1959).

Results for E_i and ν_i from the K200DB test series are given in Table 5.8. The average indirect Young's modulus was 34100 MPa and the average indirect value for Poisson's ratio is 0.372. The actual deformation moduli determined from uniaxial compressive testing were: 40100 MPa and 0.218. For the 42mm diameter samples the average indirect Young's modulus is 15% lower than the average compressive values. The indirect method of calculating Poisson's ratio overestimates the average Poisson's ratio derived from compression testing by 70%.

Table 5.5: K300DB test data at low stress level (10 MPa)

Sample	ν_c	Ec (MPa)	σ_1 (MPa)	ε_a	ε_l	Et (MPa)	ν_t	E_i (MPa)	ν_i
K302DB	0.233	35800	10.424	398.8	247.6	19300	0.599	29300	0.363
K305DB	0.214	46500	9.980	255.5	131.5	38600	0.489	41700	0.219
K306DB	0.214	46500	9.906	246.0	139.5	35000	0.351	44100	0.288

Table 5.6: K300DB test data at high stress level (20 MPa)

Sample	ν_c	Ec (MPa)	σ_1 (MPa)	ε_a	ε_l	Et (MPa)	ν_t	E_i (MPa)	ν_i
K302DB	0.249	37000	16.225	618.1	443.3	16200	0.537	30700	0.504
K305DB	0.214	44000	20.952	596.5	371.5	25900	0.446	39400	0.365
K306DB	0.214	44000	20.248	542.0	378.0	24100	0.293	43300	0.474

Table 5.7: Mean indirect tensile modulae for K300DB test series

Sample	Ec (MPa)	ν_c	Et (MPa)	ν_t	E_i (MPa)	ν_i
K302DB	36400	0.236	17750	0.568	30000	0.434
K305DB	45250	0.214	32250	0.468	40550	0.292
K306DB	45250	0.214	29550	0.322	43700	0.381

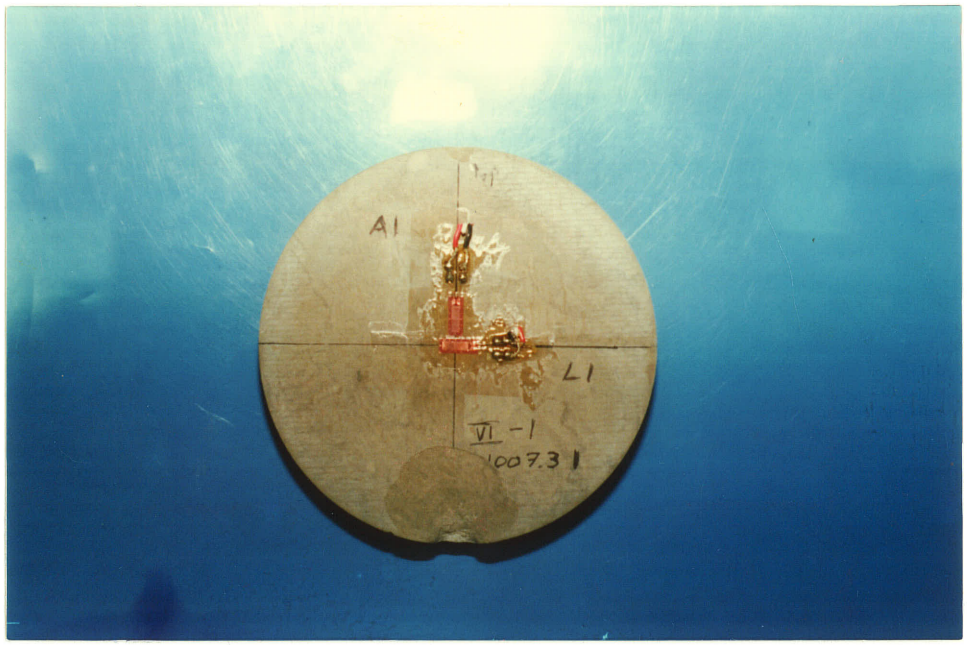

Fig. 5.4: Standard strain gauge arrangement on 89mm Brazilian sample

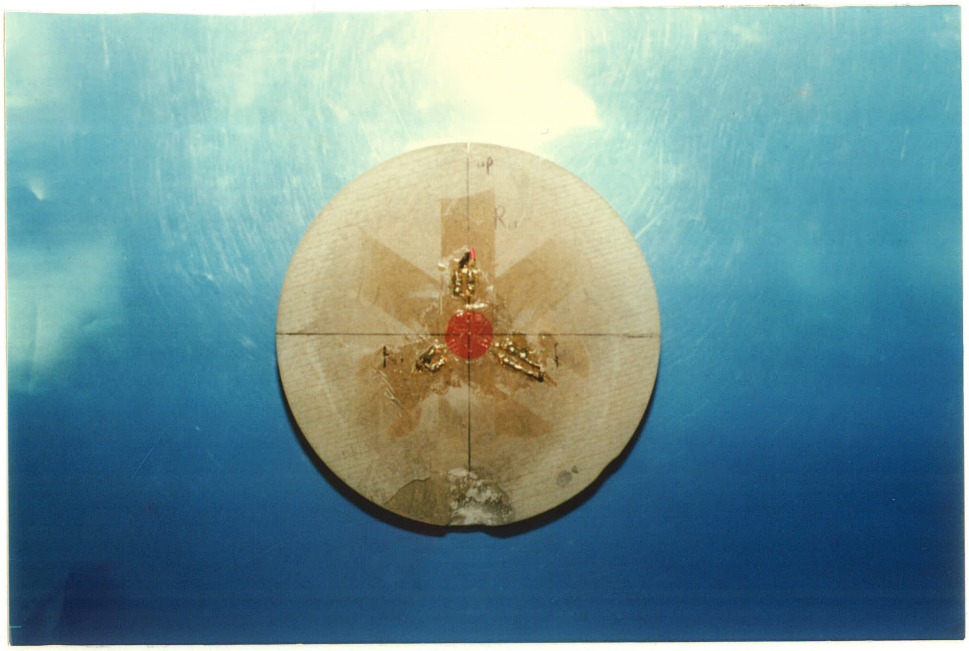

Fig. 5.5 Strain rosette arrangement on the other side of the same Brazilian sample

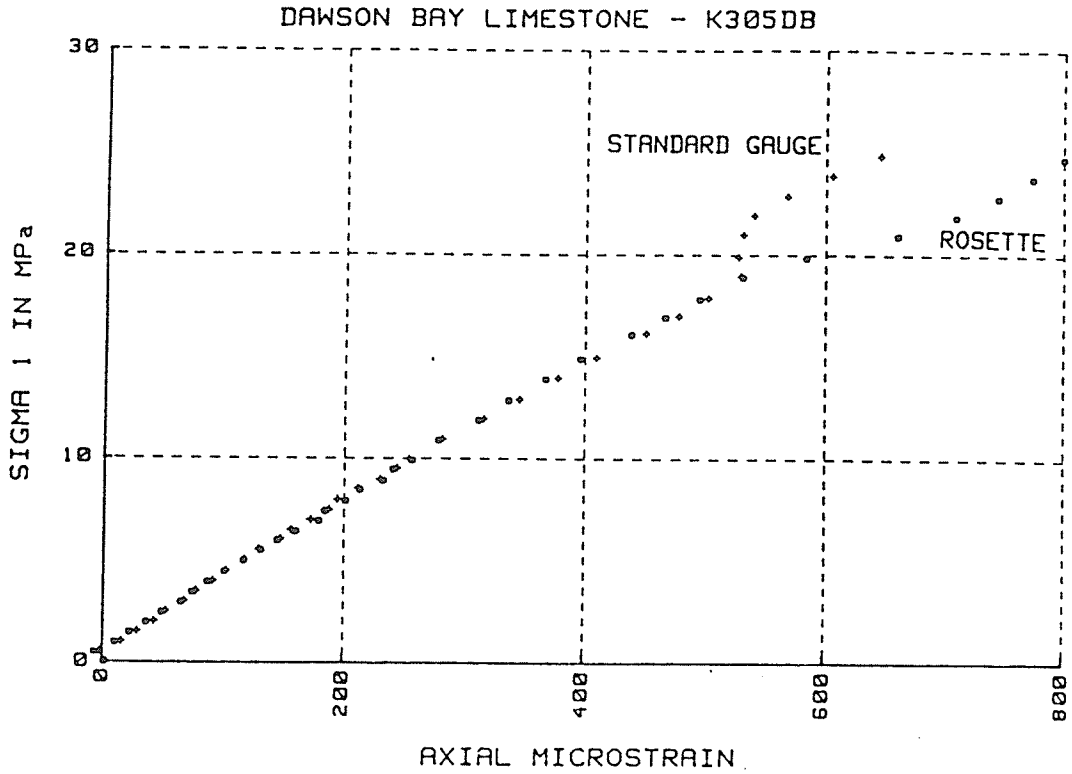

Fig. 5.6 Both the standard strain gauge arrangement and strain rosette give the same values for axial or compressive strain

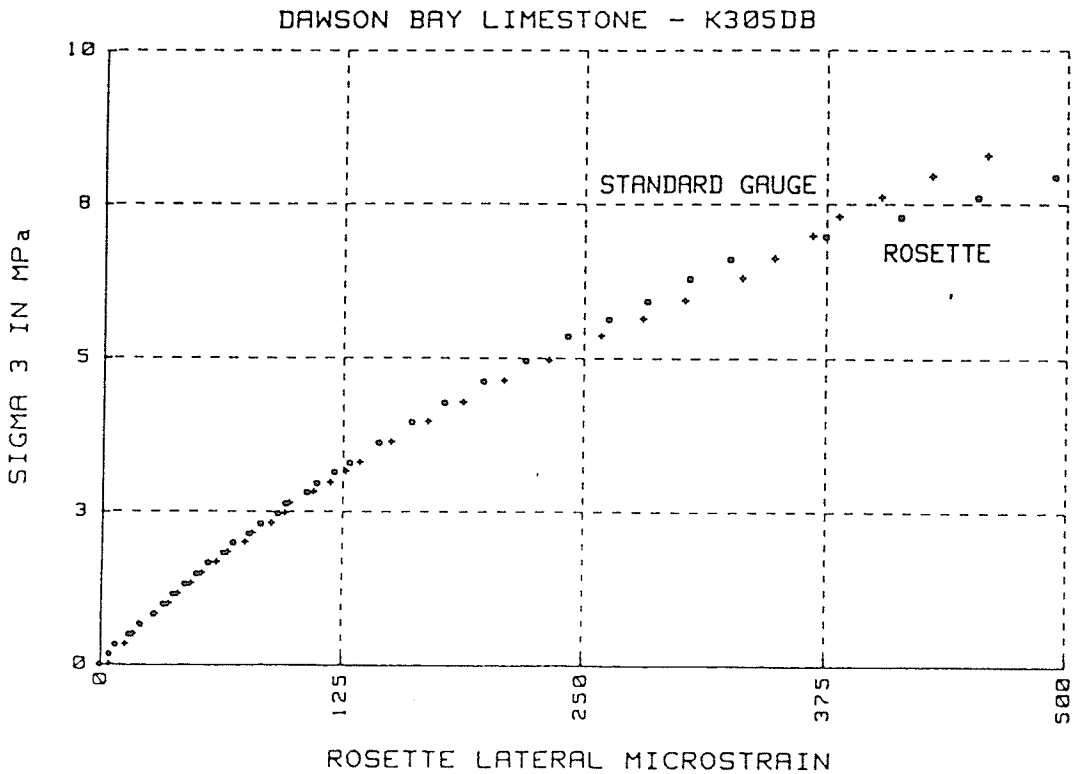

Fig. 5.7 Both the standard strain gauge arrangement and the strain rosette give similar values for the lateral or tensile strain

Results from the K300DB Brazilian test series (89mm diameter samples) are closer to the compressive results (See Table 5.9). The average indirect deformation moduli were 38400 MPa and 0.290. The average values from the uniaxial compressive tests are 42900 MPa and 0.220. In this experimental series, the indirect means of calculating Poisson's ratio overestimates the direct method by about 24%.

From the results from these two test series using two different sample sizes, one can conclude that sample size is clearly a dependent variable in the indirect method of determining compressive deformation moduli. For both the 42mm and the 89mm samples, the value for the indirect Young's modulus was only 12 - 15% lower than the direct values. In calculating the Poisson's ratio, however, the error of overestimation was reduced from 70% to 24% when using the larger diameter samples. Hondros developed these equations for an elastic, homogeneous, isotropic material and assumed in his derivations that the deformation moduli were the same in both tension and compression. From the Brazilian tests we know this is not the case for Dawson Bay Limestone, so we can not expect the indirect values to be exactly equal to the values determined by uniaxial compressive testing. It is interesting to note how much lower the error of overestimation is when the larger diameter samples are used. This is due to the more accurate measurement of tensile strain at the centre of the disk in the larger samples using the relatively smaller strain gauges. Jaeger and Cook suggest that because the stresses vary through the disk, errors may arise from the use of gauges with a finite length. They also suggest that the gauge length should therefore be confined to a length less than one tenth of the disk radius for accuracy

within a few percent. This condition was satisfied using the 89 mm disks with the strain rosettes.

Table 5.8: Indirect compressive deformation moduli from the K200DB test series

STRESS LEVEL	E_c (MPa)	ν_c	E_i (MPa)	ν_i
Low (10 MPa)	41500 (10300)	.211 (0.041)	35900 (11700)	.348 (.227)
High (20 MPa)	38700 (10700)	.225 (.037)	32400 (11100)	.396 (.266)
Average	40100	.218	34100	.372

Table 5.9: Indirect compressive deformation moduli from the K300DB test series

Sample	ν_c	E_c (MPa)	σ_c (MPa)	ε_a	ε_l	E_i (MPa)	ν_i
K302DB	0.249	37000	16.225	618.1	443.3	30700	0.504
K305DB	0.214	44000	20.952	596.5	371.5	39400	0.365
K306DB	0.214	44000	20.248	542.0	378.0	43300	0.474

CHAPTER 6

DISCUSSION

6.1 TEST RESULTS FROM OTHER SOURCES

Three other groups were involved with the investigation of the geomechanical properties of the Dawson Bay Formation. These groups were the Mining Department at Queen's university, the Canada Centre for Mineral and Energy Technology (CANMET), and the Saskatchewan Department of Mineral Resources. The results obtained by these researchers are presented in reports by DeSouza (1985), Gorski (1985), and Dunn (1982) respectively.

6.1.1 Results from Queen's University

The work done by DeSouza (1985) consisted of 90 uniaxial tests, 14 triaxial tests, and 236 Brazilian tests for a total of 340 tests. The samples used by DeSouza were all 42 mm in diameter and were obtained from five boreholes located at the Central Canada Potash mine in Colonsay, Saskatchewan. The inclination of the holes are given in Table 6.1. All uniaxial and triaxial samples were prepared having a length to diameter ratio of 2:1 and were machined to within acceptable tolerances. Confining pressure for the triaxial tests ranged from 3.4 MPa to 20.7 MPa. Brazilian disks ranged in thickness from 3.8 mm to 8.9 mm. DeSouza used the average failure angle of these tests to determine the average friction angle according to the equation:

$$A = 2 \times (T - 45) \qquad (6.1)$$

where: A = angle of internal friction
T = angle of failure plane

A plot of all the test results including average uniaxial and Brazilian

Table 6.1: Inclination of boreholes used as sample sources for Queen's test program

Borehole	Inclination from the horizontal
84-2	53
84-3	55
84-5	unknown
84-9	43
85-9	68

Table 6.2: Summary of Queen's test results

Stratigraphic Unit	σ_c (MPa)	σ_t (MPa)	E_c (MPa)	ν_c	ϕ Degrees	Cohesion (MPa)
Dawson Bay Limestone	124+/-25	11+/-2.8	30200+/-11200	0.12+/-0.06	71+/-2.6	21
First Red Beds	64+/-7	7+/-1.4	17200+/-1400	0.08+/-0.02	-----	-----
Second Red Beds	41+/-7	-----	17700+/-2800	0.17+/-0.08	-----	-----

values on a axial stress (S1) vs. confining stress (S3) graph was used to estimate the cohesion of the rock. A summary of all the Queen's testing is given in Table 6.2.

6.1.2 Results from CANMET

The work done by Gorski (1985) consisted of 32 uniaxial, 34 triaxial, 56 Brazilian, and 13 deflection tests. All the tests were performed on core provided by the Central Canada Potash Corporation from borehole 84-2. Based on geology and texture, Gorski separated the core into six units as described in Table 6.3. All uniaxial and triaxial samples were 42 mm in diameter and had a length to diameter ratio of 2:1. Each triaxial specimen was tested using a stiff testing machine at a confining pressure of 0.103, 1.03, 10.34, 20.68, and 27.58 MPa. Both the peak and residual values were obtained. Brazilian tensile strength samples were prepared with length to diameter ratios of 1:2. Deflection test samples were prepared with length to diameter ratios in excess of 3.3:1. The triaxial data was evaluated using the Hoek and Brown failure criterion for intact rock. Results from the uniaxial, triaxial and Brazilian tests are given in Table 6.4. Table 6.5 summarizes the average values for the Dawson Bay Limestone and First and Second Red Beds.

6.1.3 Saskatchewan Energy and Mines

Some limited geomechanical testing was also conducted by Dr. W. Potts, (formerly of the Saskatchewan Dept. of Mineral Resources) and was published by Dr. Colin Dunn (1982) from the Saskatchewan Dept. of Mineral Resources. The testing was conducted at the University of Saskatchewan, (U of S) and consisted of fifteen uniaxial and fifteen

Table 6.3: Unit classification of 84-2 core by CANMET (Gorski, 1986)

Geological Classification	Footage Interval (ft)	Unit
2nd Red Bed	44.0-46.0	1
Grey dolomitic mudstone	50.0-52.0	2
Grey fine grained lms.	58.0-149.2	3
Brown sugary bituminous lms.	152.6-157.8	4
Grey f.g. lms. halite filled	175.1-179.5	5
Brown sugary lms.	181.5-182.5	6

Table 6.4: Mine rock strength test results (Gorski, 1986)

Rock Type	σ_c (MPa)	σ_t (MPa)	E (MPa)	ν	m	s
Unit 1	24	3	12000	----	15.3	1
Unit 2	44	6	9000	0.15	----	-
Unit 3	128	9	41000	0.16	13.1	1
Unit 4	56	5	30000	0.3	14.2	1
Unit 5	105	9	36000	0.28	9.8	1
Unit 6	43	3	18000	0.28	8.2	1

Table 6.5: Summary of uniaxial and Brazilian test results by CANMET (Gorski, 1986)

Unit	σ_c (MPa)	σ_t (MPa)	E (MPa)	ν
Dawson Bay Limestone	119+/-45	8.89+/-2.67	38800+/-10930	0.27+/-0.05
First Red Bed	43	3+/-0.01	18000	0.28
Second Red Bed	24	3	12000	-----

tensile tests. Uniaxial compressive samples were approximately 40 mm in diameter with a height to diameter ratio of 2.1:1. The Brazilian specimens were cut from the 40 mm core with a diameter to height ratio of approximately 4. Steel loading platens for diametral compression were cemented at the extremities of the diameter in each specimen. Loading was then applied until the specimen failed. The results of the testing by the University of Saskatchewan on the Dawson Bay Limestone are summarized below.

Uniaxial compressive strength	=	207	+/-	50 MPa
Brazilian tensile strength	=	15	+/-	2.9 MPa
E in compression	=	45,900	+/-	13,700 MPa
ν in compression	=	0.222	+/-	0.06

6.2 COMPARISON OF RESULTS

A comparison of results from all sources is summarized in Table 6.6. The table shows that the U of M, CANMET and Queen's results are similar for uniaxial compressive strength (σ_c) , Brazilian tensile strength (σ_t) and Young's modulus of elasticity in compression (E_c). The three sources differ, however, on the value for Poisson's ratio in compression (ν_c). The U of M value of 0.253 and the CANMET value of 0.27 are almost identical, but the Queen's value is lower by about 50% being 0.12. The author therefore concludes that there was an error in either data acquisition or data manipulation by DeSouza resulting in a low value for ν_c. The value for Poisson's ratio obtained by the U of S is similar to those by CANMET and the U of M, however, the uniaxial compressive strength is about 75% higher than the average of the others, the Brazilian strength is 50% higher than the average of the others, and the Young's modulus in compression is 33% higher than the average value of

Table 6.6: Comparison of test results from different researchers on the Dawson Bay limestone

Source	σ_c (MPa)	σ_t (MPa)	E (MPa)	ν
U of M	110+/-41	9.39+/-2.56	34100+/-11000	.253+/-.06
CANMET	119+/-45	8.89+/-2.67	38800+/-10930	.270+/-.05
Queen's	124+/-25	11.0+/-2.80	30200+/-11200	.119+/-.05
U of S	207+/-50	15.3+/-2.94	45900+/-13700	.222+/-.06

the other sources.

The reason for this discrepancy is unclear. Certainly, because Queens, CANMET, and the U of M used the same core source, they should obtain the same results, which they do. According to sample descriptions, all workers used 42 mm diameter core for specimens, and used similar testing techniques. The orientation of the core samples were the same for the U of M, CANMET, and Queen's. The tests conducted at the U of S, however, were performed on core that was oriented at an angle of 90 degrees to the vertical. The condition of the U of S core is unknown.

A plausible explanation for this discrepancy is that there was something wrong with either the calibration factor used for the loading machine at the University of Saskatchewan, or in the calculations used to determine the compressive and tensile strengths. A problem with the calibration factor is a good explanation because the Poisson's ratio of the material is similar to that obtained by CANMET and the U of M. Poisson's ratio is calculated by dividing the lateral strain by the axial strain. A general trend exists in the Dawson Bay limestone in which the Poisson's ratio increases with the Young's modulus of elasticity. If the elasticity obtained from the U of S samples were indeed different from the other sources, one would also expect an increase in Poisson's ratio for Dawson Bay limestone.

6.3 INDIRECT TENSILE TEST RESULTS

The results from the indirect tensile moduli tests were very encouraging. In both the 42 mm Brazilian samples and the 89 mm Brazilian samples, the Young's modulus in tension was about one third lower than the Young's modulus in compression. In the K300DB test series, the Poisson's ratio in tension was about 105% higher than ν_c. In the K200DB series, the Poisson's ratio in tension was about 127% higher than ν_c. What was quite evident, however, was that the tensile deformation moduli were extremely stress dependent as shown in Figures 6.1 and 6.2. Figure 6.1 shows that the Young's modulus in tension changes from 76500 at a very low stress level to 22300 at high stress levels. Figure 6.2, shows that the Poisson's ratio in tension increases from -7.03 at very low stress levels to 0.430 at high stress levels. The Poisson's ratio in tension seems to reach a limiting value of about 0.435 at the higher stress range and remains around that value until failure occurs.

Changes of tensile elastic deformation moduli with stress have also been noted in tests on sandstone by Pandy and Singh (1986). They noted that the slope of stress taken tangent from the low to high stress levels, decreased from 16000 MPa to 2000 MPa. They also observed that Poisson's ratio changed quickly with stress level.

Changes in compressive elastic deformation moduli with stress level were less pronounced because the method of analysis used to determine the elastic moduli was to determine the slope of the stress/axial-strain curve. The limestone behaved almost elastically resulting in a near linear stress/strain relationship and consequently

near constant deformational moduli results.

The results indicate that at high stress levels, E_t is lower than E_c. This has also been observed by Jaeger and Cook.

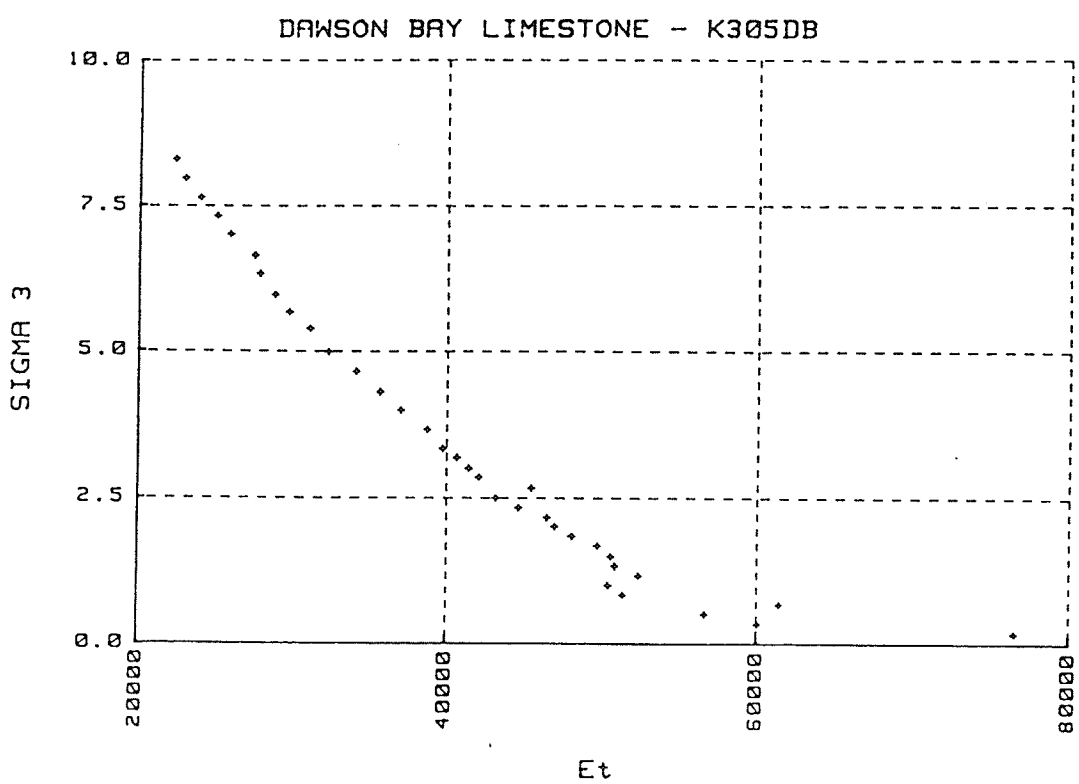

Fig. 6.1 Variation of Young's modulus of elasticity in tension with tensile stress

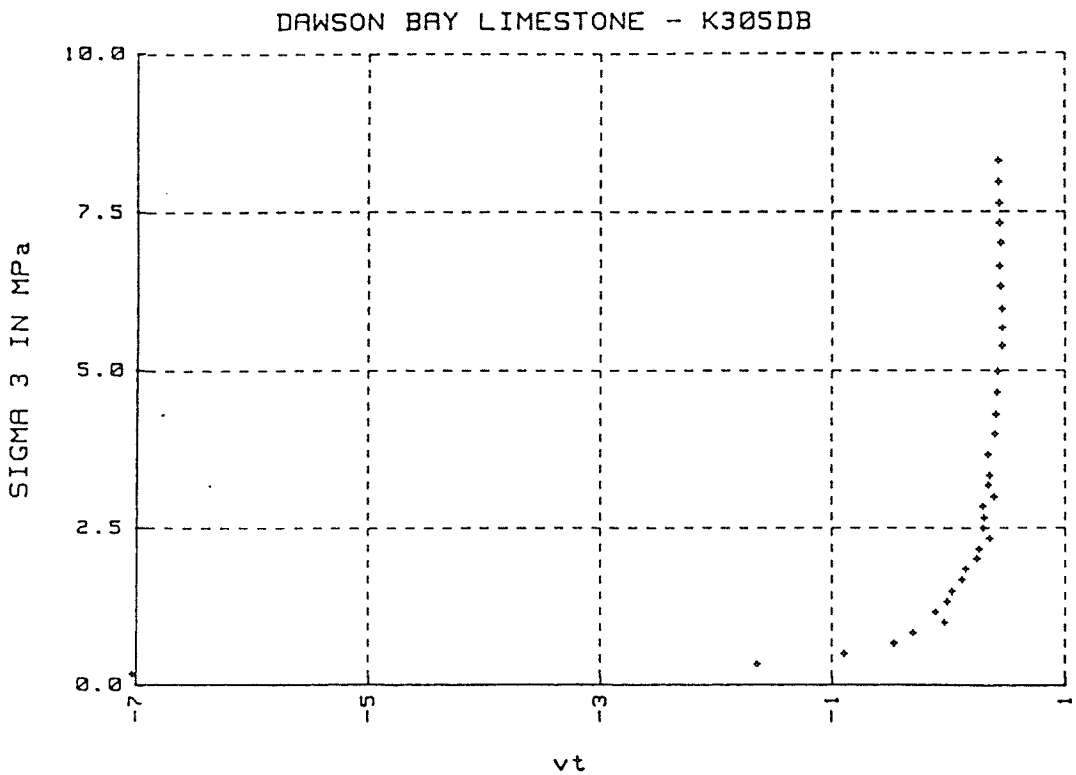

Fig. 6.2 Variation of Poisson's ratio in tension with tensile stress

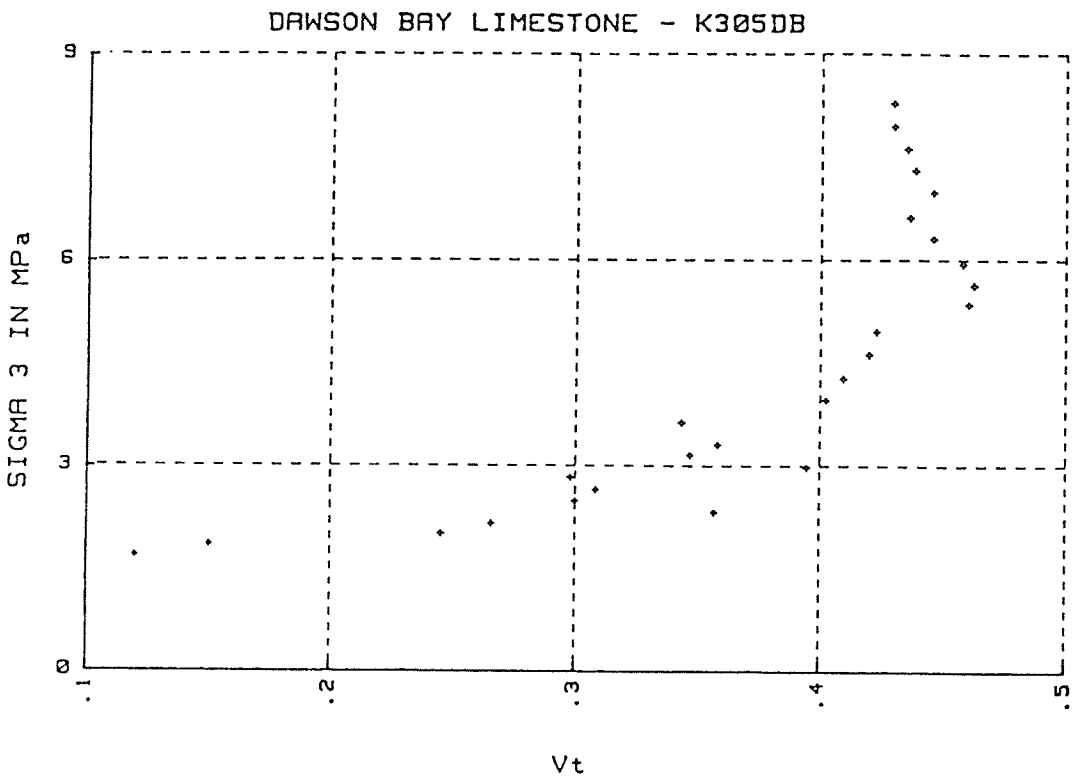

Fig. 6.3 Variation of Poisson's ratio in tension with tensile stress (smaller scale)

6.4 STATIC FATIGUE RESULTS

The value of 20 MPa as a stress limit below which no time dependent failure will occur in saturated Dawson Bay Limestone seems quite low. It is even lower than the static fatigue limit of 33 MPa for Tyndal limestone (Schmitdke, 1986) though its uniaxial compressive strength of 115 MPa is greater than that of Tyndal limestone (76 MPa). This can be explained by examining the structure of each limestone. Tyndalstone is characterized by a lack of sorting of grains and little visible pore space. It is also highly mottled and dolomitized. The Dawson Bay limestone is characterized by an extremely fine grained matrix with abundant fossils throughout. In some places the limestone is composed totally of reefoid material making it highly porous. These pores were all salt infilled. Even though a saturated brine was used in the Dawson Bay test program, salt was still leached from the pores.

Potash mine operators do not extend into areas in which the Dawson Bay limestone is wet for fear that a fracture zone might exist in the formation at that location and serve as a potential mechanism for mine flooding. In addition to this concern, it is suggested by this research that because of the reduction in strength of the limestone with water, the mine operators should also be concerned about the possible reduction in limestone strength caused by the presence of a wet zone.

6.5 STRUCTURAL MODELLING OF THE DAWSON BAY FORMATION

From the geomechanical investigations and the stratigraphic and structural well logging by the author and Dunn (1982), it is apparent that the Dawson Bay limestone is a very strong competent member. Of the cores examined by the author, only a few contained vertical to subvertical fractures. However, most of the fractures were healed or infilled with halite. The rock quality designation for the limestone members approaches 100 %, establishing the members in the VERY GOOD designation in the Hoek and Brown rock mass quality designation. The limestone members of the Dawson Bay Formation should therefore be modeled as a single thick beam 40 m in thickness with no intermittent beds of weakness.

Conversely, the Second Red Bed member is very broken up, contains abundant slickensides and in some places has a RQD of 0. This member should therefore be modeled as a weak cohesionless layer.

6.6 RECOMMENDATIONS FOR FUTURE TESTING

The basic geomechanical properties of the Dawson Bay limestone have been investigated, and enough tests have been conducted to confidently establish the: compressive, Brazilian tensile, and triaxial strengths. The Young's modulus in compression and Poisson's ratio in compression have also been well established as has the angle of direct shearing resistance. There are, however, several more areas of interest which deserve investigation:

1) Post yield strength

2) Establishment of tensile moduli by direct uniaxial tensile tests

CHAPTER 7

CONCLUSIONS

The following conclusions have been drawn with regard to the geomechanical properties of the Dawson Bay limestone.

Uniaxial compressive strength	= 110	MPa
Uniaxial compressive strength (Point load)	= 142	MPa
Brazilian tensile strength	= 9.8	MPa
Young's modulus in compression	= 34100	MPa
Poisson's ratio in compression	= 0.25	
Friction angle	= 33	deg.

Triaxial strength

Brown limestone: $\sigma_1 = \sigma_3 + \sqrt{(8.14 * 44.14 * \sigma_3 + 44.14^2)}$

Grey limestone : $\sigma_1 = \sigma_3 + \sqrt{(25.96 * 80.78 * \sigma_3 + 80.78^2)}$

The point load test results, converted to equivalent compressive strength values, were higher than the results obtained from uniaxial testing by about 27%, but are still within one standard deviation of the uniaxial compression test results.

The time dependent strength of the limestone was also examined and was found to be extremely variable. The time to failure, stress relationships that were observed were:

$$\mathrm{Ln}\ (\sigma_L) = -4.370 + (\mathrm{Ln}\ 60 - .1 \times \mathrm{Ln}\ (t))$$

$$\mathrm{Ln}\ (t) = -43.8 + 10 \times \mathrm{Ln}\ (60/\sigma_L)$$

A static fatigue limit of 20 MPa was also determined, below which no time dependent failure of the limestone would occur.

Two different sizes of Brazilian samples were used in the indirect tensile deformation moduli experimentation, and each displayed its own distinct mode of failure. The 42 mm diameter "thick" disks failed in tension with a vertical crack down the centre. The 89 mm "thin" disks

"thin" disks failed by spalling of the faces. The average value for the Young's modulus in tension was not affected by the difference in sample diameter and is approximately one third less than that in compression. Determination of Poisson's ratio is diameter dependent, with ν_t 105% higher than ν_c for the 89 mm samples and ν_t 127% higher than ν_c for the 42mm samples. The elastic moduli obtained from the 89 mm tests are probably closest to the true value.

The Dawson Bay limestone members should be modelled as a single thick elastic beam 40 m thick with vertical fractures. Due to the variability of the results from the geomechanical test program, a sensitivity approach should be used, employing the upper and lower as well as the average strength values. The Second Red Bed member should be modeled as a weak cohesionless layer 4.2 m thick.

REFERENCES

Barton, N.R. (1971). "A relationship between joint roughness and joint shear strength". Rock Fracture Proc. of Int. Symp. on Rock Mech., Nancy, France.

Beer, F.P. and Johnston, E.R. (1981). "Mechanics of Materials". McGraw-Hill Book Company.

Bieniawawski, Z.T. and Hawkes I. (1978). "Suggested methods for determining tensile strength of rock materials - ISRM commission on standardization of laboratory and field tests". Int. J. Rock Mech. Min. Sci., Vol.15. pp. 99-103.

Broch E. and Franklin J.A. (1972). "The Point load test". Int. J. Rock Mech. Min. Sci., Vol. 9, pp. 669-697.

Brook, Norman (1977). "The use of irregular specimens for rock strength tests". Int. J. Rock Mech. Min. Sci., Vol. 14, pp. 193-202.

CANMET (1977). "Determination of point load strength index". in: Pit Slope Manual, Supplement 3-1, Laboratory Classification tests.

Deere, D.U. (1964). " Technical description of rock cores for engineering purposes." Rock Mechanics and Engineering Geology. Vol. 1, No. 1, pp. 17-22.

DeSouza, E. (1985). "Rock Mechanics laboratory tests - Dawson Bay, lrst Red Beds, 2nd Red Beds". Unpublished report, Department of Mining, Queen's University.

Dunn, C.E. (1982). "Geology of the Middle Devonian Dawson Bay Formation in the Saskatoon potash mining district, Saskatchewan. Sask. Energy and Mines, Rept. 194.

Gadi, A.M. (1986). "Creep along a discontinuity in granite". Unpublished M.Sc. thesis, Department of Civil Engineering , University of Manitoba.

Gendzwill D.J. (1983). "Elastic properties of carbonate rocks over the Cory mine". Potash '83 Proceedings, Pergamon Press.

Gorski, B. (1985). "Strength determinations of Central Canada Potash rocks". Unedited interm report, Minerals Research Program Mining Research Laboratories Division Report MRP/MRL 85-124(INT), CANMET.

Hoek, E. and Brown, E.T. (1980). "Underground excavations in rock", Institution of Mining and Mettalurgy, London.

Hondros, G. (1959). "The evaluation of Poisson's ratio and modulus of materials of low tensile resistance by the Brazilian test with particular reference to concrete." Aust. J. Applied Sci., Vol. 10, pp. 243-268.

Horner, R.B. (1983). "Earthquakes in Saskatchewan: A potential hazard to the potash industry". Potash '83 Proceedings, Pergamon Press.

Jaeger, J.C. and Cook, N.G.W. (1969). "Fundimentals of Rock Mechanics". Fletcher and Son Ltd., Norwich, London.

Kroll, D.W. (1985). "Introduction to the geology and geomechanical properties of the Dawson Bay Formation". Unpublished inhouse report, Dept. Civil Engineering, University of Manitoba.

Kroll, D.W. (1986). "Basic geomechanical properties of the carbonate members of the Dawson Bay Formation". Unpublished inhouse report, Dept. Civil Engineering, University of Manitoba.

Lajtai, E.Z. and Schmidtke, R.H. (1986). "Delayed failure in rock loaded in uniaxial compression". Rock Mech and Rock Eng., Vol. 19, No. 1, pp. 11-26.

Mellor, M. and Hawkes, I. (1971). "Measurement of tensile strength by diametral compression of discs and annuli". Eng. Geol., 5, pp. 173-225.

ROCTEST (1985). "Point load tester model PIL-5 instruction manual". Roctest Ltd.

Schmidtke, R.H. (1986). "The strength and static fatigue of a granite, an anorthosite and a limestone". Unpublished M.Sc. Thesis, Department of Civil Engineering, University of Manitoba.

Snowden, W.E. (1977). "Surface flaws and the mechanical behaviour of glass optical fibres". In: Fracture Mechanics of Ceramics 3, Bradt R.C., Hasselman D.P.H., Lange F.F. (Eds.).

Weibull W. (1951). "A statistical distribution function of wide applicability". Applied Mechanics Reviews 5, pp. 449-451.